Animal Nutrition 17 (2024) 265–282

Contents lists available at ScienceDirect

Animal Nutrition

journal homepage: http://www.keaipublishing.com/en/journals/aninu/

Original Research Article

Development and application of a multi-step porcine in vitro system to evaluate feedstuffs and feed additives for their efficacy in nutrient digestion, digesta characteristics, and intestinal immune responses

Hee Yeon Kim [b], Jun-Ok Moon [b], Sung Woo Kim [a, *]

[a] Department of Animal Science, North Carolina State University, Raleigh, NC, USA
[b] Application Center, CJ Blossom Park, Suwon, South Korea

ARTICLE INFO

Article history:
Received 25 September 2023
Received in revised form
9 January 2024
Accepted 17 January 2024
Available online 4 March 2024

Keywords:
Digestion
Feed additive
Feedstuff
In vitro
Intestine
Pig

ABSTRACT

In vitro model provides alternatives to the use of live animals in research. In pig nutrition, there has been a tremendous increase in in vivo research over the decades. Proper utilization of in vitro models could provide a screening tool to reduce the needs of in vivo studies, research duration, cost, and the use of animals and feeds. This study aimed to develop a multi-step porcine in vitro system to simulate nutrient digestion and intestinal epithelial immune responses affected by feedstuffs and feed additives. Seven feedstuffs (corn, corn distillers dried grains with solubles [corn DDGS], barley, wheat, soybean meal, soy protein concentrates, and *Corynebacterium glutamicum* cell mass [CGCM]), feed enzymes (xylanase and phytase), and supplemental amino acids (arginine, methionine, and tryptophan), were used in this in vitro evaluation for their efficacy on digestibility, digesta characteristics, and intestinal health compared with the results from previously published in vivo studies. All in vitro evaluations were triplicated. Data were analyzed using Mixed procedure of SAS9.4. Evaluations included (1) nutrient digestibility of feedstuffs, (2) the effects of feed enzymes, xylanase and phytase, on digestibility of feedstuffs and specific substrates, and (3) the effects of amino acids, arginine, tryptophan, and methionine, on anti-inflammatory, anti-oxidative, and anti-heat stress statuses showing their effects ($P < 0.05$) on the measured items. Differences in dry matter and crude protein digestibility among the feedstuffs as well as effects of xylanase and phytase were detected ($P < 0.05$), including xylo-oligosaccharide profiles and phosphorus release from phytate. Supplementation of arginine, tryptophan, and methionine modulated ($P < 0.05$) cellular inflammatory and oxidative stress responses. The use of this in vitro model allowed the use of 3 experimental replications providing sufficient statistical power at $P < 0.05$. This indicates in vitro models can have increased precision and consistency compared with in vivo animal studies.
© 2024 The Authors. Publishing services by Elsevier B.V. on behalf of KeAi Communications Co. Ltd. This is an open access article under the CC BY-NC-ND license (http://creativecommons.org/licenses/by-nc-nd/4.0/).

1. Introduction

With an increased global consumption of pork, pig nutrition research has become one of the most extensively researched areas in animal science. The number of peer-reviewed papers in pig nutrition increased by 10 folds from 95 papers in 1975 to 963 papers in 2020 (Kim and Duarte, 2021), indicating a dramatic increase in swine nutrition research. This may be related to continuous genetic improvement requiring re-evaluation of nutrient requirements, continuous advances in management practices, allowing new feeding strategies, and increased health concerns influencing nutritional status of pigs.

Among more than 200 abstracts presented in the area of pig nutrition at the American Society of Animal Science conference held in 2022 (ASAS, 2022a; ASAS, 2022b), topics on traditional nutrition research made up 58% whereas research related to intestinal health accounted for 42% of the presentations, indicating a

* Corresponding author.
E-mail address: sungwoo_kim@ncsu.edu (S.W. Kim).
Peer review under responsibility of Chinese Association of Animal Science and Veterinary Medicine.

Production and Hosting by Elsevier on behalf of KeAi

https://doi.org/10.1016/j.aninu.2024.01.006
2405-6545/© 2024 The Authors. Publishing services by Elsevier B.V. on behalf of KeAi Communications Co. Ltd. This is an open access article under the CC BY-NC-ND license (http://creativecommons.org/licenses/by-nc-nd/4.0/).

big increase in research related to intestinal health. When the topics were classified by research areas, amino acid nutrition, mineral nutrition, evaluation of feed enzymes, and impacts of prebiotics and probiotics covered more than 60% (Fig. 1). All these 200 research presentations were from studies using animals. Thus, the need for in vitro nutrition research models is obvious. In vitro studies reduce research cost by eliminating the need for animals and feeds whilst greatly reducing the length of time required to conduct the experiment. In vitro techniques are extensively used to evaluate the digestibility of feedstuffs and with the effect of feed additives for pigs (Boisen and Fernández, 1995; Regmi et al., 2009; Woyengo et al., 2016) and poultry (Bryan et al., 2018; Weurding et al., 2001; Zaefarian et al., 2021) with known limitations. In the case of the in vitro digestion model, accumulation of end-products can limit digestion process (Greiner, 2021; Mandalari et al., 2009). In vitro cell culture or tissue culture models do not consider complex regulation and interaction among various cell types and tissues within an animal body (Vinyard and Faciola, 2022).

In vitro studies have also been used to simulate the intestinal immune system (Bouffi et al., 2023; Roh et al., 2022) and its responses to microbial and viral challenges (Chen et al., 2017; Lock et al., 2022; Tsamandouras et al., 2017; Zhang et al., 2022). In vitro models can be utilized as a tool for screening candidates of feed additives prior to in vivo animal studies. Various attempts have been made to screen feed additives on rumen methane mitigation (Bodas et al., 2008; Durmic et al., 2014; Parra et al., 2023), showing promising potential for the approach to be applied in porcine models.

Intestinal health is a critically important issue in pig nutrition especially in newly weaned pigs (Jha and Kim, 2021; McCracken et al., 1999). In recent years, there have been a dramatic increase in developing feed additives to improve intestinal health of newly weaned pigs (Jang and Kim, 2022; Kim and Duarte, 2021; Zheng et al., 2021). Intestinal health of nursery pigs is closely associated with the intestinal immune system and its responses including alterations in mucosa-associated microbiota (Duarte and Kim, 2022; Xu et al., 2022), inflammatory responses (Cheng et al., 2021; Duarte et al., 2019; Jang et al., 2023), and oxidative damages (Chen et al., 2020; Deng et al., 2023a; Moita et al., 2021a) in the jejunal mucosa of nursery pigs.

This study hypothesized that a multi-step porcine in vitro system for the simulation of nutrient digestion and intestinal cell responses can be used as a tool to screen feed additives for their efficacy prior to animal studies. Seven feedstuffs (corn, corn distillers dried grains with solubles [corn DDGS], barley, wheat, soybean meal, soy protein concentrates, and *Corynebacterium glutamicum* cell mass [CGCM]), feed enzymes (xylanase and phytase), and supplemental amino acids (arginine, methionine, and tryptophan), were used in this in vitro evaluation for their efficacy on digestibility and intestinal health compared with the results from previously published in vivo studies.

2. Materials and methods

2.1. Animal ethics statement

This study did not use live animals and thus animal ethics certificate was not required to carry out the in vitro evaluation.

2.2. Materials

Feed enzyme (xylanase and phytase), protein supplements (soybean meal and soy protein concentrates), and supplemental amino acids (arginine, methionine, and tryptophan) were used in this multi-step porcine in vitro system. This in vitro system is the CJ BIO Animal Nutrition and Health Application Platform designed and developed by CJ Blossom Park (Suwon, Republic of Korea) to simulate nutrient digestion and intestinal cell responses of multi-animal species including pigs, poultry, and cattle. The multi-step porcine in vitro system includes 2 application parts: "the gastrointestinal tract (GIT) application" simulating nutrient digestion and "the Cell application" simulating intestinal cell responses. Xylanase (endo-β-1,4-xylanase) was obtained from CJ BIO (Seoul, Republic of Korea). The genetic information of xylanase was originated from *Orpinomyces* PC2 and the enzyme was produced using *Trichoderma reesei*. The activity of xylanase (XU) was measured by determining the amount of enzyme required to release 1 μmol xylose equivalence from 1% beechwood or sugarcane bagasse per minute at 50 °C and pH 6.5 (Manfredi et al., 2015) and the measured activity was used to provide 50,000 XU/g. Phytase (6-phytase, 88,000 FTU/g) was obtained from CJ BIO. The genetic information of phytase was originated from *Escherichia coli* and the enzyme was produced using *T. reesei*. The activity of phytase (FTU) was measured by determining the amount of phytase that liberates 1.0 μmol of inorganic phosphorus per minute at 40 °C and pH 5.5 (Moita and Kim, 2023) and the measured activity was used to provide 88,000 FTU/g. *C. glutamicum* cell mass was obtained from CJ BIO (Seoul, Republic of Korea). Soybean meal was obtained from a local supplier (DH Vital Feed, Pyeongtaek, Republic of Korea) containing 48% CP and 3.0% lysine. Soy protein concentrate was obtained from CJ Selecta (Araguari, MG, Brazil) containing 64% CP and 3.9% lysine (Deng et al., 2022). Corn and wheat were obtained from a local supplier (DH Vital Feed, Pyeongtaek, Republic of Korea) and corn DDGS and barley were obtained from CJ F&C (Seoul, Republic of

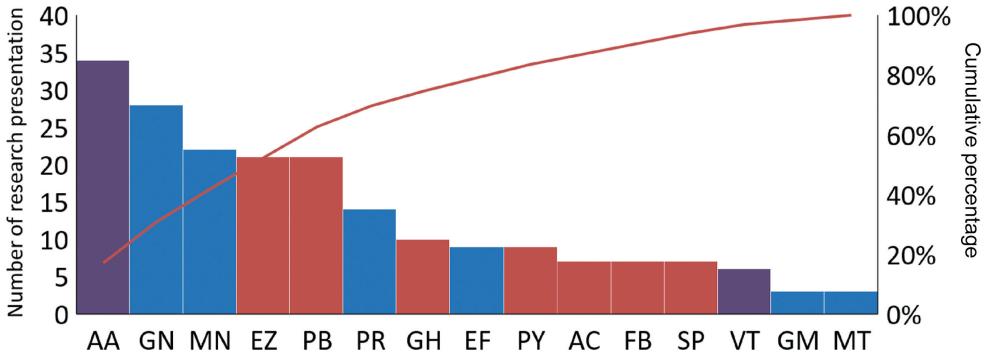

Fig. 1. Topic areas of research abstracts in the area of pig nutrition presented at the American Society of Animal Science conferences held in 2022. Data were obtained from ASAS (2022a, 2022b). AA = amino acids; AC = acidifiers; EF = energy and fats; EZ = enzyme; FB = fiber; GH = gut health; GM = general management; GN = general nutrition; MN = mineral; MT = mycotoxins; PB = pre-, pro-, post-biotics; PR = protein; PY = phytogenics; SP = soy protein; VT = vitamins.

Korea). Arginine (98.5% L-arginine) and tryptophan (60% L-tryptophan, Trp GC) used in this study were obtained from CJ BIO. Three types of methionine were used in this study: L-methionine (99%, CJ BIO), D-methionine (98%, M9375, Sigma Aldrich, St. Louis, MO, USA), and DL-methionine (99%, M2768, Sigma Aldrich, St. Louis, MO, USA). A multi-step porcine in vitro system was used to determine digestibility of nutrients (the GIT application) and intestinal epithelial or immune cell responses (the Cell application).

2.3. The GIT application: artificial gastrointestinal model for nutrient digestibility

The artificial gastrointestinal model (Fig. 2) developed by the Application Center of CJ Blossom Park (Suwon, Republic of Korea) was used to measure in vitro digestibility of various feedstuffs affected by xylanase and phytase. The artificial gastrointestinal model consists of 12 digestion chambers, 12 feeding pumps, 2 cooling chambers, 12 coolant lines, 4 heating chambers, 12 heating water line, and a computing system. Figure 3 shows one of 4 units. Each unit has 3 digestion chambers.

The digestion chamber is made of a double jacketed reaction flask (Pyrex glass, 1.1 L capacity) equipped with head stirrer (impeller), pH meter, thermometer, feeding pump line, and water circulator (BIOCNS, Daejeon, Republic of Korea). Figure 4 shows a photo of the digestion chamber. During the digestion step, stirring of the digesta is controlled by an impeller (0 to 2000 rpm) and the temperature is controlled (20 to 60 °C) by circulating water between the space of double jacketed glasses. During the digestion step, a buffer is provided (27 mL/min) through the feeding pump line (range: 0 to 65,000 mL/min). The entire process can be programmed and automated by a software program (CIMONX, CIMON, Sungnam, Republic of Korea) and the representing screen captures the in vitro digestion steps as shown in Fig. 5.

2.3.1. In vitro digestion

In vitro digestion was carried out using the artificial gastrointestinal model and the each digestion process had a 360-min cycle. Firstly, triplicate samples of corn DDGS, soybean meal, and CGCM were used to evaluate the digestibility of dry matter and crude protein. Secondly, the effects of xylanase on digestibility of nutrients in selected feedstuffs were tested. Five feedstuffs commonly used in swine feeds were evaluated including corn, wheat, barley, soybean meal (48% CP), and corn DDGS with or without xylanase (4 XU/kg). Each feedstuff (with or without xylanase) was replicated 6 times for the evaluation of in vitro digestibility (3 replicates) and digesta viscosity (3 replicates). All tested feedstuffs were ground with a commercial blender (HMF-3250S, Hanil Electric, Bucheon, Republic of Korea) to particle size to pass 1-mm screen following the procedure by Boisen and Fernández (1997). Thirdly, the efficacy of phytase on hydrolysis of phytate and the composition of phytic acids were measured.

To the first step simulated stomach digestion: 20 g of each feedstuff (with or without xylanase) was added in the digesta with 0.1 mol/L phosphate buffer (pH 2.5, 370 mL) with 0.3% pepsin (Choi et al., 2021) and maintained for 2 h at 39 °C with continuous stirring at 700 rpm (Boisen and Fernández, 1997; Jean and Yolande,

Fig. 2. The artificial gastrointestinal model with 12 digestion chambers (CJ Blossom Park, Suwon, Republic of Korea).

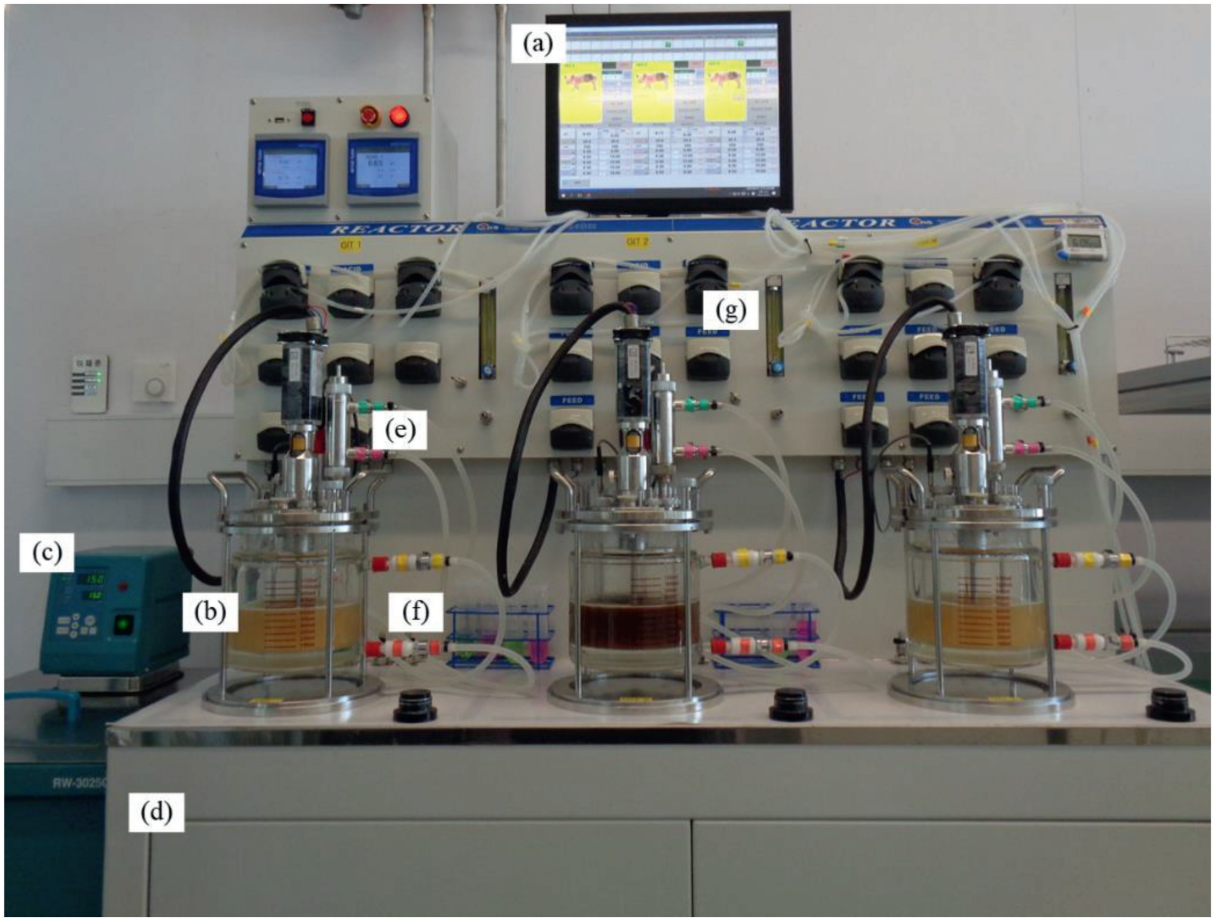

Fig. 3. A close view of a part of the artificial gastrointestinal model: (a) control panel (computing system), (b) digestion chamber (doubled jacketed reaction flask), (c) cooling chamber, (d) heating chamber, (e) coolant line, (f) heating water line, and (g) feeding pumps.

2007; Regmi et al., 2009). To the second step simulated small intestinal digestion: 0.2 mol/L phosphate buffer (pH 6.8, 100 mL) and 0.4 mol/L NaOH (50 mL) were added at pH 6.8; consequently, 0.8% pancreatin (20 mL, Sigma Aldrich, St. Louis, MO, USA) was added and the digestion was maintained for 4 h at 39 °C with continuous stirring at 700 rpm (Boisen and Fernández, 1997; Jean and Yolande, 2007; Regmi et al., 2009).

2.3.2. Digestibility of dry matter and crude protein

After the completion of a 2-step digestion, 3 digesta replicates were filtered through Nylon mesh (30 μm, Narae Plus, Seoul, Republic of Korea) and the filtrates were dried at 60 °C for 24 h in a drying oven (NB-901M, N-BIOTEK, Bucheon, Republic of Korea). The weights of dried samples before the digestion (a), filter (Nylon mesh) (b), samples with filter after the digestion, filtration, and drying (c) were obtained after drying at 105 °C for 4 h (Method 934.01, AOAC, 2007), and used to calculate dry matter digestibility (%) following the equation by Boisen and Fernández (1995):

$$\text{Dry matter digestibility (\%)} = [(a + b - c)/(a + b)] \times 100.$$

For the determination of CP digestibility (%), dried filtrate (25 mg) was used in an Elemental Analyzer (vario MACRO cube, Elementar, Hesse, Germany) for the quantification of nitrogen (Biancarosa et al., 2017). The analyzed nitrogen content was multiplied by 6.25 to obtain the crude protein content (Marco et al., 2002). Crude protein digestibility (%) was calculated following the equation:

$$\text{Crude protein digestibility (\%)} = \{c - [a \times (1 - b)]\}/c \times 100,$$

where a = CP in the dried filtrate (%); b = DM digestibility; and c = CP in the sample (%).

2.3.3. Digesta viscosity of feedstuffs with or without xylanase

Samples digesta (25 mL) were taken from the remaining 3 digestion chambers at different time points (0, 10, 60, 120, 240, and 360 min) during the second step of the model. Obtained digesta were centrifuged at 2800 × g (5810R, Eppendorf, Hamburg, Germany) at 20 °C for 15 min (Ayres et al., 2019). Supernatants (5 mL) were transferred to 25 mL Falcon tubes, frozen at −80 °C, and freeze dried (LP03, Ilshin BioBase, Yangju, Republic of Korea). Freeze-dried sample was dissolved in distilled water (0.5 mL) and used to measure viscosity. Viscosity was measured using a viscometer (DV2T, Brookfield, MA, USA). A sample (500 μL) was loaded to a viscometer under 20 and 50 rpm at 39 °C for 20 s (Bedford and Classen, 1993; Moita et al., 2022; Passos et al., 2015). The changes of viscosity from 0 to 360 min of the second step digestion were plotted using the time as an independent variable (x-axis) and the viscosity (cP) as a dependent variable (y-axis). The area under the curve was calculated (Graphpad Prism 5 software) and compared between treatments (with or without xylanase) following Cheryl et al. (2006).

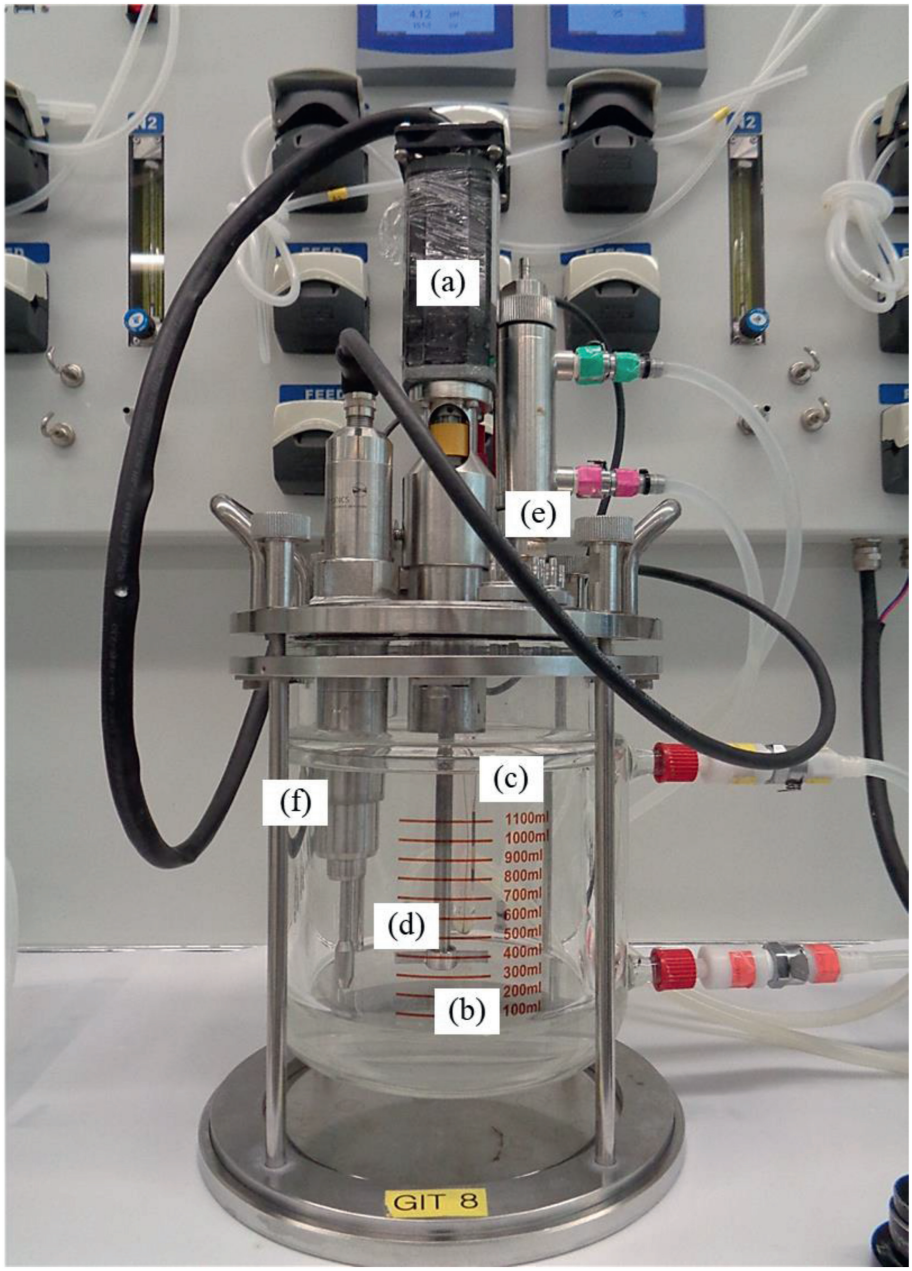

Fig. 4. A close view of a digestion chamber: (a) head stirrer, (b) impeller, (c) pH meter, (d) thermometer, (e) feeding pump line, and (f) continuous viscometer. GIT = the gastrointestinal tract.

2.3.4. Separation and quantification of xylo-oligosaccharides (XOS) in digesta from feedstuffs with or without xylanase

Digesta obtained from the in vitro digestion were further used to separating and quantifying XOS following the procedure of Folch et al. (1957). Digesta (1 mL) were diluted with distilled water (4 mL), and then diluted digesta (1 mL) was mixed with methanol (1.33 mL) and chloroform (2.66 mL) with vortexing. Mixed digesta samples were centrifuged at 1580 × *g* and 20 °C for 3 min (5810R, Eppendorf, Hamburg, Germany). Supernatant (0.5 mL) was transferred into a microcentrifuge tube (3810X, Eppendorf, Hamburg, Germany) and frozen at −80 °C. Frozen samples were dried to remove solvent by a centrifugal vacuum concentrator (HyperVAC-LITE, Hanil Scientific Inc., Gimpo, Republic of Korea) at 35 °C for 4 h.

Dried samples were dissolved in 0.5 mL 50% methanol and filtered through a C8 cartridge (Sep-Pak C8 Vac RC, Waters, MA, USA) and then a 0.22-μm syringe filter (AS031320-19, Agela Technologies, CA, USA). Filtered samples (2 μL) were used to separate and quantify XOS using liquid chromatography–mass spectrometry following De Leoz et al. (2013). A liquid chromatography (UPLC, Acquity Premier UPLC System, Waters, MA, USA) with a column at 35 °C (2.1 mm × 150 mm, Acquity UPLC BEH Amide, Waters, MA, USA) and a mass spectrometry detector (Xe-vo TQ-XS, Waters, MA, USA) were used. Two mobile phases were used: (1) 80% acetonitrile (ACN) with 0.1% ammonia solution (AmOH, 5.43830, Sigma Aldrich, St. Louis, MO, USA) and (2) 30% ACN with 0.1% AmOH. The gradients of 80% ACN:30% ACN were set at 40:60 (0 to 10 min) and 100:0 (10 to 20 min) with the flow rate was set at 0.17 mL/min. The positive electrospray ionization (ESI) mode was used for ionization with capillary voltage at 2.8 kV and cone voltage at 25 V (Kouzounis et al., 2022).

Fig. 5. The screen captures of the digestion steps showing the program and the automated process of the artificial gastrointestinal model. (A) The first step of the in vitro digestion to simulate stomach digestion. (B) The second step of the in vitro digestion to simulate the small intestine. GIT = the gastrointestinal tract.

2.3.5. Quantification of phosphorus release from phytate with or without phytase

Phytic acid solution (10 mmol/L) was prepared by dissolving 0.28 g phytic acid (P8810, Sigma Aldrich, St. Louis, MO, USA) in 40 mL distilled water at pH 2.0 (Hirvonen et al., 2019). Phytase (200 FTU/mL) was prepared by adding 0.02 g phytase (88,000 FTU/g) to 8.8 mL sodium acetate buffer (0.25 mol/L at pH 5.5) followed by incubation using a shaking incubator (VS-8480, Vision Scientific,

Daejeon, Republic of Korea) at 200 rpm and 39 °C for 30 min. It was further diluted 10× with 0.25 mol/L sodium acetate buffer (pH 5.5) to obtain phytase with 20 FTU/mL.

For the first step of digestion, 100 μL phytase (20 FTU/mL) was added to 10 mL phytic acid solution (10 mmol/L) with 0.3% pepsin (250 units/mg, P7000, Sigma Aldrich, St. Louis, MO, USA) and digested at 39 °C and spun at 200 rpm for 2 h in 3 replicates (Boisen and Fernández, 1997; Jean and Yolande, 2007; Regmi et al., 2009). During the digestion, samples (1 mL) were taken at 0, 30, 60, and 120 min and the samples were immediately heated using a heat block (MS-100, AllSheung, Hangzhou, China) at 95 °C for 10 min. Digesta samples were filtered using 0.22-μm syringe filter (Agela Technologies, CA, USA) and the filtrates were used for the second step of digestion. The pH of filtrate was adjusted to 6.5 by adding 0.45 mL NaOH (1 mol/L), mixed with 0.6 mL of 20% pancreatin (P1750, Sigma Aldrich, St. Louis, MO, USA) in distilled water, and digested at 39 °C and 200 rpm for 4 h in 3 replicates (Boisen and Fernández, 1997; Jean and Yolande, 2007; Regmi et al., 2009). During the digestion, samples (1 mL) were taken at 0, 2, and 4 h and the samples were immediately heated using a heat block (MS-100, AllSheung, Hangzhou, China) at 95 °C for 10 min. The digesta samples were filtered using a 0.22-μm syringe filter (Agela Technologies, CA, USA) to collect filtrates.

The filtrates from digesta samples were used for the quantification of phosphorus using a colorimetric assay. First, the dye reagent was prepared by mixing a dye reagent concentrate with a nitric acid solution (100 mL, 22%, 5617-4400, Daejung, Siheung, Republic of Korea), a solution (50 mL) with ammonium hydroxide (0.25%, 1065-4410, Daejung, Siheung, Republic of Korea) and ammonium molybdate (10%, 1073-4400, Daejung, Siheung, Republic of Korea), and an ammonium metavanadate solution (50 mL, 0.235%, 1072-4105, Daejung, Siheung, Republic of Korea).

The standard used for the phosphorus quantification was prepared dissolving 0.05 mol/L potassium phosphate monobasic (6613-4400, Daejung, Siheung, Republic of Korea) into 0.25 mol/L sodium acetate buffer (pH 5.5) to achieve 0, 313, 625, 1250, 2500, and 5000 nmol.

Filtered digesta samples or the standard (0.1 mL) were mixed with 2 mL dye reagent, and 2.9 mL acetate buffer (0.25 mol/L at pH 5.5), and incubated at room temperature for 10 min. After the incubation, the mixture was centrifuged (1696R, Labogene, Lillerød, Denmark) at 2800 × *g* for 5 min. The supernatants were taken and used to measure color intensity (optical density) using a spectrophotometer (UV-1800, SHIMADZU, Kyoto, Japan) at 415 nm (Kitson and Mellon, 1944).

The amounts of phosphorus in the filtered digesta samples and the standard were calculated based on the following equation:

$$\text{Phosphorus release (\%)} = (b/a) \times 100,$$

where *a* is phosphorus in the standard; and *b* is phosphorus in the sample.

2.4. The Cell application: intestinal cell model for immune status

2.4.1. Cell culture

Intestinal porcine epithelial cells (IPEC-J2, DSMZ No. ACC701, BWE, Germany) were seeded in T75 cell culture flasks (70075, SPL Lifesciences, Gyeonggi-do, Republic of Korea) and cultured with Dulbecco's Modified Eagle Medium/Nutrient Mixture F-12 (DMEM/F12, Thermo Fisher Scientific, Waltham, MA, USA) containing 10% fetal bovine serum (FBS, SV30207.02, Hyclone, Cytiva, Australia), 1% insulin–transferrin–selenium–ethanolamine (ITS-X, 51500056, Thermo Fisher Scientific, Waltham, MA, USA) and 1% penicillin–streptomycin (15140-122, Thermo Fisher Scientific, Waltham, MA, USA) at 37 °C in a humidified atmosphere with 5% CO_2 (Li et al., 2022; Yan and Ajuwon, 2017). Cells were sub-cultured once every 3 to 4 d (twice a week) until the confluence reached 90%. For the sub-culture, cells were detached from the flask by Trypsin/EDTA (GIBCO, NY, USA), centrifuged at 300 × *g* for 3 min, re-suspended and re-seeded at concentration of 5.0×10^5 cells in 25 mL of complete cell culture medium per T75 flask (Fig. 6).

Bone marrow-derived macrophages (BMDM) were obtained from porcine tibia or femur bones (21-d-old pigs) with the presence of growth factors. The femurs were cut at both ends with sterile scissors. The bone marrow was flushed out using 18-gauge needle and 10 mL syringe filled with ice-cold Dulbecco's Modified Eagle Medium (DMEM, Thermo Fisher Scientific, Waltham, MA, USA) onto a 70 μm nylon cell strainer (Model 352350, Corning Incorporated, NY, USA) and placed in a 50 mL conical tube (SPL Lifesciences, Gyeonggi-do, Republic of Korea). Cells were centrifuged at 300 × *g* for 5 min and the supernatant was removed (Liu and Quan, 2015; Toda et al., 2020; Weischenfeldt and Porse, 2008). The 5 mL of red blood cell lysis buffer (Thermo Fisher Scientific, Waltham, MA, USA) was added and allowed to stand for 5 min. The 40 mL of cell medium containing 1% penicillin–streptomycin was added and strained through the cell strainer (Model 352350, Corning Incorporated). Cells were centrifuged at 300 × *g* for 5 min and the supernatant was removed again. Isolated cells were cultured with DMEM containing 5% FBS and mM-CSF (416-ML-010, R&D systems, MN, USA) at 37 °C in a humidified atmosphere with 5% CO_2 (Gao et al., 2018; Na et al., 2016).

2.4.2. Cell viability

To evaluate the cytotoxicity of samples to IPEC-J2, cells were seeded in 96-well plates (Corning Incorporated, NY, USA) at 1.5×10^4 cells per well. After overnight incubation at 37 °C with 5% CO_2, the wells were washed by DMEM/F-12 and treated with the medium containing various amounts of test samples (arginine at 0 to 5000 mg/L, tryptophan at 0 to 2500 mg/L, and methionine at 0 to 5000 mg/L) for 24 h. After the incubation period, wells were washed using DMEM/F-12 and diluted WST-1 working solution (10× WST reagent, EZ-3000, DOGEN Bio, Gyenggi-do, Republic of Korea) was added (100 μL) to each well (Weir et al., 2011). After incubating for 2 h, the absorbance at 450 nm was determined by a microplate reader (Epoch 2, BioTek, Winooski, VT, USA).

$$\text{Cell viability (\%)} = (OD_{450} \text{ of treated cells}/OD_{450} \text{ of untreated cells}) \times 100,$$

where OD_{450} is optical density at 450 nm.

2.4.3. Inflammatory status

To establish the inflammatory status in IPEC-J2 cell line, the expression of mRNA for interleukin 8 (*IL8*) was quantified. Briefly, cells were seeded at 1.0×10^5 cells/well (1 mL per well) in 24-well plates and cultured overnight. Cells were pre-treated with or without test samples for 18 h and challenged with 1 μg/mL of deoxynivalenol (DON, D0156, Sigma Aldrich, St. Louis, MO, USA) (DON/control, test sample + DON/treated group) for 3 h (Xu et al., 2020).

After these treatments, cells were washed with cold phosphate-buffered saline (PBS) and harvested for the total RNA extraction and the quantification of *IL8* mRNA. The test samples were arginine (0 vs. 2500 mg/L), tryptophan (0, 50, and 100 mg/L), and methionine (0 vs. 2500 mg/L). The percent reduction of *IL8* was calculated following the equation below:

$$\text{Reduction (\%)} = [(\text{RGE of challenged cells} - \text{RGE of pretreated and challenged cells})/\text{RGE of challenged cells}] \times 100,$$

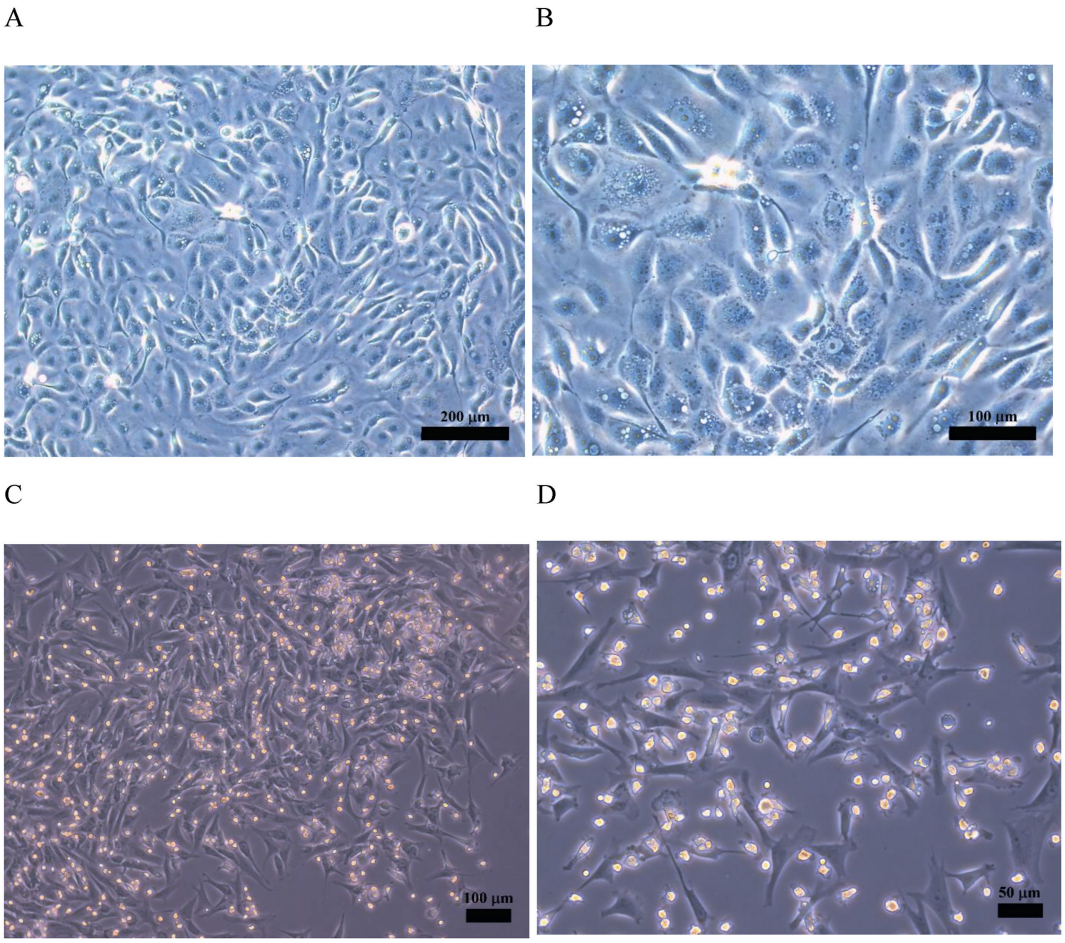

Fig. 6. Cultured cells under the microscope. (A) Intestinal porcine epithelial cells (IPEC-J2) at 100× magnification. Scale bar, 200 μm. (B) IPEC-J2 at 200× magnification. Scale bar, 100 μm. (C) Bone marrow-derived macrophages (BMDM) at 100× magnification. Scale bar, 100 μm. (D) BMDM at 200× magnification. Scale bar, 50 μm.

where RGE is relative gene expression.

To establish the anti-inflammatory status in BMDM, IL10 was quantified. Briefly, isolated cells were cultured for 5 d. There were 5.0×10^5 cells/well in a 48-well plate including DMEM medium supplemented with 5% FBS and 20 ng/mL mM-CSF and differentiated (Na et al., 2016). Cells were incubated with test samples for 20 h. The test samples were methionine (0 vs. 2500 mg/L) and tryptophan (0 vs. 100 mg/L).

Cell culture supernatants were collected, centrifuged at 16,000 × *g* for 3 min, and stored at −80 °C until the quantification of anti-inflammatory cytokine, IL10. The concentration of IL10 was determined using the Duoset ELISA kit (DY693B, R&D systems, MN, USA). The standard was used in a working range between 0 and 1500 pg/mL. A 96-well microplate was coated with 100 μL/well of the capture antibody (4 μg/mL) and incubated at room temperature overnight. Each well was aspirated and washed with washing buffer 3 times. The plate was blocked by adding 300 μL Reagent diluent to each well, incubated at room temperature for 1 h and washed. The 100 μL samples and standards in Reagent diluent were added, incubated for 2 h and washed. The 100 μL the detection antibody (50 ng/mL) was added, incubated for 2 h and washed. The 100 μL streptavidin-horseradish peroxidase (HRP) was added, incubated for 20 min, and washed. The 100 μL substrate solution was added and incubated for 20 min. The reaction was stopped by adding 50 μL stop solution. The absorbance at 450 nm was determined by a microplate reader and IL10 concentration was expressed as pg/mL.

2.4.4. Oxidative stress status

To establish the oxidative stress status in IPEC-J2 cell line, the amount of total reactive oxygen species (ROS) was quantified. Briefly, cells were seeded at 1.5×10^4 cell/well (100 μL per well) in a 96-well plate. After overnight incubation at 37 °C, cells were pre-treated with or without test samples for 18 h and then washed by Hank's Balanced Salt Solution (HBSS, 14175095, Thermo Fisher Scientific, Waltham, MA, USA). To determine the amount of ROS, cells were incubated with 10 μM 2′,7′-dichlorofluorescin-diacetate (DCF-DA, D6883, Sigma Aldrich, St. Louis, MO, USA) for 30 min and then treated with 0.5 mmol/L H_2O_2 for 30 min (Vergauwen et al., 2015). The fluorescence was read at 485 nm for excitation and 530 nm for emission with a fluorescence microplate reader (BioTek Synergy H1). The test samples were arginine (0 vs. 2500 mg/L), tryptophan (0, 50, and 100 mg/L), and methionine (0 vs. 5000 mg/L). The percent reduction of ROS was calculated as follows:

Reduction (%) = [(RFU of challenged cells − RFU of pretreated and challenged cells)/RFU of challenged cells] × 100,

where RFU is relative fluorescence units.

2.4.5. Heat stress status

To establish the heat stress status in IPEC-J2 cell line, the expression of mRNA for heat shock protein 70 (*HSP70*) was quantified. Briefly, IPEC-J2 cells were seeded at 4.0×10^5 cell/well in a 6-well plate and cultured at 37 °C for 24 h. Cells pre-treated with or

without test samples for 18 h were divided into two groups: (1) the control group (exposure to 37 °C for 2 h) or (2) the HS group (exposure to 42 °C for 2 h); and then cells were cultured at 37 °C for 6 h (Cui et al., 2022; Zhang et al., 2023). Cells were washed with cold PBS and harvested for total RNA extraction. The test samples were arginine (0 vs. 2500 mg/L), tryptophan (0, 50, and 100 mg/L), and methionine (0 vs. 2500 mg/L). For quantification of *HSP70*, the isolated RNA was analyzed using reverse transcription quantitative polymerase chain reaction (RT-qPCR). The percent of production was calculated as follows:

HSP70 production (%) = (RE of *HSP70* in pretreated and challenged cells/RE of *HSP70* in challenged cells) × 100,

where RE is relative expression.

To establish the heat stress status in BMDM, the amount of HSP70 was quantified. Briefly, isolated cells were cultured for 5 d. There were 1×10^6 cell/well in a 24-well plate including DMEM medium supplemented with 5% FBS and 20 ng/mL mM-CSF and differentiated. Cells pre-treated with or without test samples for 18 h were divided into two groups: (1) the control group (exposure to 37 °C for 2 h) or (2) the HS group (exposure to 42 °C for 2 h); and then cells were cultured at 37 °C for 20 h. The test samples were arginine (0 vs. 2500 mg/L), tryptophan (0, 50, and 100 mg/L), and methionine (0 vs. 2500 mg/L).

The cell pellet was collected, rinsed with PBS, and lysed using the radioimmuno-precipitation assay (RIPA) lysis and extraction buffer (89900, Thermo Fisher Scientific, Waltham, MA, USA) at 4 °C for 15 min. The supernatants were stored at −80 °C until the quantification of HSP70 proteins. The HSP70 concentration was determined using the Pig Heat Shock Protein 70 ELISA Kit (MBS702042, Mybiosource, BC, Canada). The 100 μL sample and standard were added to microplate wells coated with capture antibody and incubated at 37 °C for 2 h. The 100 μL Biotin-antibody was incubated at 37 °C for 2 h. The detection occurred using 100 μL HRP, 3,3′,5,5′-tetramethylbenzidine (TMB) substrate, and a stop solution. The absorbance at 450 nm was determined using a microplate reader. The total protein concentration was determined using the BCA protein assay kit (23225, Thermo Fisher Scientific Inc., Waltham, MA, USA). The absorbance was measured at 562 nm. The HSP70 concentration was expressed as ng/μg protein. The percent of production was calculated as

$$\text{HSP70 production (\%)} = \left(\frac{\frac{\text{HSP70 conc.}}{\text{protein conc.}} \text{ in pretreated and challenged cells}}{\frac{\text{HSP70 conc.}}{\text{protein conc.}} \text{ in challenged cells}} \right) \times 100,$$

where the concentration of HSP70 is ng/mL and the concentration of protein is μg/mL.

2.4.6. Cell proliferation

To establish cell proliferation, IPEC-J2 were seeded at 1.5×10^4 cells/mL (100 μL per well) in 96-well plates. The test samples were diluted to twice the desired final concentration (2 folds) in the cell media and 100 μL/well was added to each well. The 20 μL of a 5′-bromo-2′-deoxyuridine reagent (500×, BrdU cell proliferation kit 2750, Sigma Aldrich, St. Louis, MO, USA) was added and incubated for 24 h to determine the relative proliferation of the cells. Test sample was tryptophan (0, 50, and 100 mg/L).

To detect the BrdU label by the anti-BrdU monoclonal antibody, cells were fixed by 200 μL of fixing solution, reacted for 30 min and washed 3 times by 300 μL washing solution. The 100 μL of anti-BrdU monoclonal antibody was added, incubated at room temperature for 1 h and washed. The goat anti-mouse IgG, peroxidase conjugate, was filtered by a 0.22-μm syringe filter, added to each well and reacted for 30 min. The TMB peroxidase substrate was added and incubated for 30 min. The reaction was stopped by the acid stop solution. The absorbance at 450 nm was determined by a microplate reader (Yin et al., 2014).

Cell proliferation (%) = (OD_{450} of pretreated cells/OD_{450} of untreated cells) × 100,

where OD_{450} is optical density at 450 nm.

2.4.7. RNA extraction and real-time PCR for IL8 and HSP70 in intestinal epithelial cells

Total RNA was extracted from IPEC-J2 using the easy-spin RNA extraction kit (17221, iNtRON, Republic of Korea). Cells were lysed by adding 1 mL lysis buffer (easy-BLUE reagent) and transferred into a 1.5 mL tube (SPL Life Sciences, Gyeonggi-do, Republic of Korea), followed by the addition of 200 μL chloroform to each tube, and then vigorously vortexed. The tubes were centrifuged at 16,000 × *g* under 4 °C for 10 min and the supernatant was then transferred into an empty 1.5-mL tube. The 400 μL binding buffer was added and mixed by pipetting or gently inverting 3 times. The 800 μL of the upper solution was loaded to the column and centrifuged at 16,000 × *g* for 1 min. The spin column was placed in the collection tube. The 700 μL washing buffer A was added to the column and centrifuged at 16,000 × *g* for 1 min (Jin et al., 2022). The column was washed by adding 700 μL washing buffer B and centrifuged at 16,000 × *g* for 1 min. The flow-through was discarded and the column was centrifuged at 16,000 × *g* for 1 min to dry the column. The column was placed in a clean 1.5 mL tube and 50 μL elution buffer was added onto the membrane. After the incubation for 1 min, the tube was centrifuged at 16,000 × *g* for 1 min to elute. The RNA purity and concentration were measured by spectrophotometry (QIAxpert System, Qiagen, Hilden, Germany).

The RT-qPCR was performed on Rotor-gene Q 2plex platform (Qiagen) in a final volume of 20 μL using the AccuPower GreenStar RT-qPCR PreMix (K-6403, Bioneer, Republic of Korea). The PCR reaction mixture contained 10 μL 2× master mix, 2 μL each primer (10 pmol/μL), 2 μL template RNA, and 4 μL DEPC-DW. The mixture was added into a PCR tube and the PCR consisted of cDNA synthesis at 50 °C for 15 min and pre-denaturation at 95 °C for 5 min, followed by 40 cycles at 95 °C for 15 s, 55 °C for 30 s, and 72 °C for 30 s. The primers were designed with Primer-Blast (https://www.ncbi.nlm.nih.gov/tools/primer-blast/) based on the published cDNA sequence in the GenBank. The relative abundance of targeted genes was calculated according to the $2^{-\Delta\Delta Ct}$ method and normalized to the mean expression of TATA box binding protein (*TBP*) or glyceraldehyde 3-phosphate dehydrogenase (*GAPDH*) serving as the internal reference gene. Information on the detected genes and primers is shown in Table 1.

2.5. Statistical analysis

Data obtained in this study were analyzed using the Mixed Procedure of SAS 9.4 (SAS Institute, Cary, NC, USA). For in vitro evaluation of nutrient digestibility and intestinal cell responses, a completely randomized design was used to test the main effects. Dietary treatments were considered fixed effects and the probability of differences (pdiff) option was used for multiple range test.

The linear and quadratic effects of increasing levels of arginine, tryptophan, and methionine in cell viability evaluation were tested by polynomial contrasts with coefficients by the Proc IML

Table 1
Primer sequences used in this study.

Gene	Primer sequences (5′–3′)	Length, bp	Access no.	Reference
IL8	F: AGCCCGTGTCAACATGACTT R: TGGAAAGGTGTGGAATGCGT	147	NM_213867.1	Primer-Blast[1]
HSPA6	F: GAATCCGCAGAATACCGTGT R: TCCGCAGTCTCCTTCATCTT	213	NM_001123127.1	Adur et al. (2022)
TBP	F: GATGGACGTTCGGTTTAGG R: AGCAGCACAGTACGAGCAA	124	XM_021085497.1	Kern et al. (2017)
GAPDH	F: GTTGTGGAGTCCACTGGTGT R: CCCATCACAAACATGGGGGC	119	NM_001206359.1	Jeong et al. (2014)

IL8 = interleukin-8; *HSPA6* = heat shock protein family A (*HSP70*) member 6; *TBP* = TATA box binding protein; *GAPDH* = glyceraldehyde-3-phosphate dehydrogenase.
[1] Primer-Blast (https://www.ncbi.nlm.nih.gov/tools/primer-blast/).

procedure of SAS 9.4. Preplanned contrasts were made to compare treatments with or without amino acids. When significant differences or tendencies were present, the data were further analyzed using the NLMIXED procedure to determine the break point to obtain the optimal supplemental level, as previously described (Jang et al., 2021; Moita et al., 2021b). The statistical significance and tendency were declared at $P < 0.05$ and $0.05 \leq P < 0.10$, respectively.

Data from phosphorus release (%) from phytate were used in slope-ratio assay according to Choi et al. (2023) and Kim and Easter (2001). The statistical model used in the analysis is according to the following equation:

$$y = a + bt \times xt + bs \times xs + e,$$

where y represents response criterion (% phosphorus release); a is an intercept (% phosphorus release); bt and bs are the slopes for phytase (0 or 200 FTU/mL); xt and xs are the time of digestion (min) with phytase (0 or 200 FTU/mL); e is the error term.

3. Results

3.1. The GIT application

3.1.1. Digestibility of dry matter and crude protein

Digestibility (%) of dry matter and crude protein in selected protein supplements (soybean meal, soy protein concentrate, corn DDGS, and CGCM) was measured and compared among tested feedstuffs (Table 2). Digestibility of dry matter in CGCM was the greatest ($P < 0.05$) and that in corn DDGS was the lowest ($P < 0.05$). Soy protein concentrate had greater ($P < 0.05$) dry matter digestibility than conventional soybean meal. Digestibility of crude protein in soy protein concentrate was greater ($P < 0.05$) than that in soybean meal and corn DDGS. Digestibility of crude protein in corn DDGS was the lowest ($P < 0.05$) among tested feedstuffs. Digestibility of crude protein in CGCM was not detectable because of insignificant residuals (dried filtrate) after digestion.

Digestibility of dry matter in selected cereal grains (corn, wheat, barley) and protein supplements (soybean meal and corn DDGS) were measured with and without xylanase (Table 3) to evaluate the effects of xylanase on the dry matter digestibility. Supplementation of xylanase (4 XU/kg) increased ($P < 0.05$) the dry matter digestibility of wheat (4.0%) and barley (2.1%), whereas the dry matter digestibility of corn, soybean meal, and corn DDGS was not affected.

3.1.2. Digesta viscosity of feedstuffs with or without xylanase

Viscosity of digesta was also measured (Table 4). Supplementation of xylanase (4 XU/kg) reduced ($P < 0.05$) the viscosity of wheat (20.7%) and barley (10.5%), and tended to reduce ($P = 0.051$) the viscosity of corn (4.2%), whereas the viscosity of soybean meal and corn DDGS was not affected.

Table 2
Digestibility of dry matter and crude protein in various feedstuffs using the artificial gastrointestinal model (%).

Digestibility	SBM	SPC	Corn DDGS	CGCM	SEM	*P*-value
Dry matter	75.3[b]	79.2[c]	50.2[a]	98.6[d]	0.56	<0.001
Crude protein	92.2[b]	95.1[c]	75.0[a]	–	0.30	<0.001

SBM = soybean meal; SPC = soy protein concentrates; corn DDGS = corn distillers dried grains with solubles; CGCM = *Corynebacterium glutamicum* cell mass.
[a–d]Means within a row lacking common superscripts differ ($P < 0.05$).

3.1.3. Separation and quantification of xylose-oligosaccharide in digesta from feedstuffs with or without xylanase

Amounts (mg/kg) of XOS with various numbers of monomers (from 2 to 6) were measured after digestion with or without xylanase (4 XU/kg) (Fig. 7). Digestion with xylanase increased ($P < 0.05$) the amount of xylotriose in corn and corn DDGS, and both xylobiose and xylotriose in soybean meal. Digestion with xylanase increased ($P < 0.05$) the amount of xylobiose, xylotriose and xylotetraose in wheat and barley. There is no xylopentaose or xylohexaose generated from the digestion of feedstuffs with xylanase.

3.1.4. Quantification of phosphorus released from phytic acid with or without phytase

The time course release of phosphorus from phytic acid after digestion with or without phytase (200 FTU/mL) is shown in Fig. 8. There was no increase of phosphorus release from phytic acid when phytase was not added in digestion. However, when phytase was added, phosphorus release linearly increased ($P < 0.05$) from 16.2% to 33.1% during the 360-min digestion.

3.2. The Cell application

3.2.1. Arginine

The viability of IPEC-J2 was evaluated by increasing the dose of arginine in culture media (Table 5). Increasing the dose of arginine

Table 3
Digestibility of dry matter in feedstuffs with xylanase (0 or 4 XU/kg[1]) using the artificial gastrointestinal model (%).

Digestibility	Xylanase, XU/kg[1]		SEM	*P*-value
	0	4		
Corn	73.3	73.4	0.24	0.627
Wheat	83.5	86.8	0.11	0.001
Barley	70.8	72.3	0.19	0.012
Soybean meal	75.4	75.3	0.12	0.479
Corn DDGS	52.3	52.7	0.22	0.292

Corn DDGS = corn distillers dried grains with solubles.
[1] XU (unit) is the amount of enzyme required to release 1 μmol xylose equivalent from 1% beechwood or sugarcane bagasse per minute at 50 °C and pH 6.5 (Manfredi et al., 2015).

Table 4
Viscosity of feedstuffs digested with xylanase (0 or 4 XU/kg[1]) using the artificial gastrointestinal model.

Viscosity, AUC[2]	Xylanase, XU/kg[1]		SEM	*P*-value
	0	4		
Corn	945	905	9.8	0.051
Wheat	2038	1616	27.4	0.001
Barley	1565	1401	11.2	0.001
Soybean meal	1615	1629	5.4	0.103
Corn DDGS	1229	1216	10.3	0.408

Corn DDGS = corn distillers dried grains with solubles.
[1] XU (unit) is the amount of enzyme required to release 1 μmol xylose equivalent from 1% beechwood or sugarcane bagasse per minute at 50 °C and pH 6.5 (Manfredi et al., 2015).
[2] AUC is the area under the curve from a plot with the time as an independent variable (x-axis) and the viscosity (cP) as a dependent variable (y-axis) following Cheryl and George (2006).

reduced ($P < 0.05$) viability of IPEC-J2 in a quadratic manner with a breakpoint ($P < 0.05$) at 2502 mg/L (Fig. 9).

Inflammatory, oxidative stress, and heat stress statuses in IPEC-J2 and BMDM with or without the inclusion of arginine at 2500 mg/L were evaluated (Table 6). Inclusion of arginine at 2500 mg/L reduced ($P < 0.05$) the production of *IL8* (27.3%) and ROS (26.8%) in IPEC-J2. However, production of *HSP70* both in IPEC-J2 and BMDM was not affected by the inclusion of arginine.

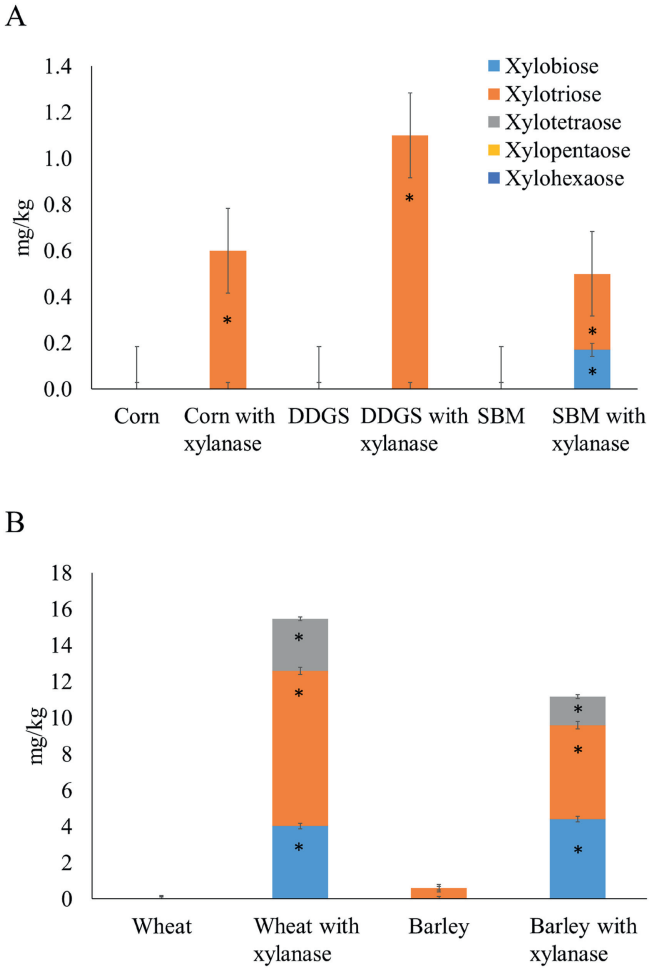

Fig. 7. Amount of xylose oligosaccharides in various length in feedstuffs (corn, DDGS, SBM, wheat, and barley) after digestion with or without xylanase (4 XU/kg): (A) corn (xylotriose; *, with vs. without xylanase: $P < 0.05$), DDGS (xylotriose; *, with vs. without xylanase: $P < 0.05$), and soybean meal (xylobiose and xylotriose; *, with vs. without xylanase: $P < 0.05$) and (B) wheat (xylobiose, xylotriose, and xylotetraose; *, with vs. without xylanase: $P < 0.05$) and barley (xylobiose, xylotriose, and xylotetraose; *, with vs. without xylanase: $P < 0.05$). DDGS = distillers dried grains with solubles; SBM = soybean meal.

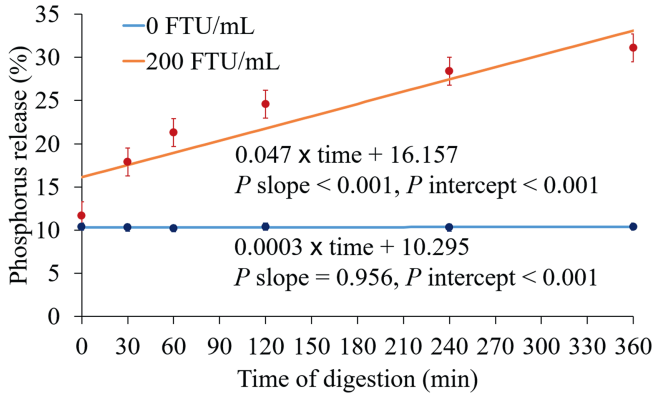

Fig. 8. Slope-ratio comparison of phosphorus release (%) from phytate with or without phytase. The slope of 0 FTU/mL and the slope of 200 FTU/mL were different ($P < 0.001$).

3.2.2. Tryptophan

The viability of IPEC-J2 was evaluated by increasing the dose of tryptophan in culture media (Table 7). Increasing the dose levels of tryptophan both linearly and quadratically reduced ($P < 0.05$) viability of IPEC-J2 with a breakpoint ($P < 0.05$) at 1006 mg/L. The breakpoint (one-slope broken-line model) was 1005.6 mg/L tryptophan when cell viability was 102% ($P < 0.05$). In the one-slope broken-line model, the equation for cell viability is $y = 102.1 - 0.064 \times z1$; if tryptophan is ≤ breakpoint, then $z1 = 0$; if tryptophan is >breakpoint, then $z1$ = tryptophan − breakpoint.

Inflammatory, oxidative stress, and heat stress statuses in IPEC-J2 and BMDM with increasing dose levels of tryptophan from 0 to 100 mg/L were evaluated (Table 8). Increasing the dose of tryptophan from 0 to 100 mg/L reduced ($P < 0.05$) *IL8* production at 50 mg/L, linearly increased ($P < 0.05$) the production of IL10 in BMDM, and linearly reduced ($P < 0.05$) the production of ROS in IPEC-J2. Increasing the dose of tryptophan from 0 to 100 mg/L linearly increased ($P < 0.05$) the production of *HSP70* in both IPEC-J2 and BMDM and also linearly increased ($P < 0.05$) proliferation of IPEC-J2.

3.2.3. Methionine

The viability of IPEC-J2 was evaluated by increasing the dose of different types of methionine (D-methionine, L-methionine, and DL-methionine) in culture media (Table 9). Increasing the dose levels of L-methionine and DL-methionine both linearly and quadratically reduced ($P < 0.05$) viability of IPEC-J2 with a breakpoint ($P < 0.05$) at 2510 mg/L. The breakpoint (one-slope broken-line model) was 2510 mg/L methionine when cell viability was 100.4% ($P < 0.05$). In the one-slope broken-line model, the equation for cell viability is $y = 100.4 - 0.005 \times z1$; if methionine is ≤breakpoint, then $z1 = 0$; if methionine is >breakpoint, then $z1$ = methionine − breakpoint.

Inflammatory, oxidative stress, and heat stress statuses in IPEC-J2 and BMDM with different types of methionine (L-methionine, D-methionine, and DL-methionine) at 2500 mg/L were evaluated (Table 10). Inclusion of L-methionine and DL-methionine at 2500 mg/L reduced ($P < 0.05$) the production of *IL8* in IPEC-J2 and the effects of L-methionine (28.5%) was greater ($P < 0.05$) than DL-methionine (18.4%) on reducing the production of *IL8*. Inclusion of L-methionine at 2500 mg/L increased ($P < 0.05$) the production of

Table 5
Viability of intestinal porcine epithelial cells (IPEC-J2) with different dose levels of arginine (Arg) (%).

Item	Arg, mg/L							SEM	*P*-value		
	0	156	313	625	1250	2500	5000		Linear	Quadratic	0 vs. Arg
Viability[1]	100.0	117.0	114.1	113.2	118.9	106.6	88.4	4.58	0.497	0.033	0.015

[1] Cell viability (%) was calculated by (OD_{450} of treated cells/OD_{450} of untreated cells) × 100, where OD_{450} is an optical density at 450 nm.

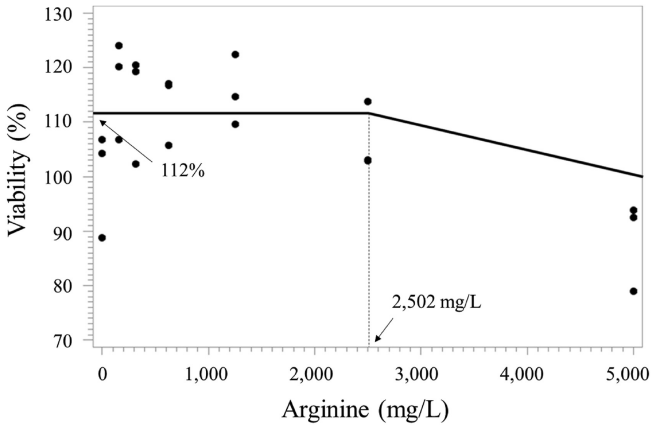

Fig. 9. A broken line analysis (graph) for the viability of intestinal porcine epithelial cells (IPEC-J2) as increasing the dose of arginine. The breakpoint (one-slope broken-line model) was 2502 mg/L arginine when cell viability was 112% ($P < 0.05$). One-slope broken-line model; the equation for cell viability is $y = 111.9 - 0.005 \times z1$; if arginine is ≤ breakpoint, then $z1 = 0$; if arginine is > breakpoint, then $z1$ = arginine − breakpoint.

Table 6
Reduction of *IL8* and ROS, and production of HSP70 in IPEC-J2 and BMDM with arginine at 2500 mg/L.

Item	Cell type	Arginine, mg/L		SEM	*P*-value
		0	2500		
IL8, % reduction[1]	IPEC-J2	0.0	27.3	2.77	<0.001
ROS, % reduction[2]	IPEC-J2	0.0	26.8	4.19	<0.001
HSP70, % production[3]	IPEC-J2	100.0	112.8	12.77	0.333
HSP70, % production[4]	BMDM	100.0	122.6	24.41	0.385

IL8 = interleukin 8; ROS = reactive oxygen species; HSP70 = heat shock protein 70; IPEC-J2 = intestinal porcine epithelial cells; BMDM = bone marrow-derived macrophages.
[1] Percent (%) of reduction was calculated by [(RGE of challenged cells − RGE of pretreated and challenged cells)/RGE of challenged cells] × 100, where RGE is relative gene expression.
[2] Percent (%) of reduction was calculated by [(RFU of challenged cells − RFU of pretreated and challenged cells)/RFU of challenged cells] × 100, where RFU is relative fluorescence units.
[3] Percent (%) of production was calculated by (RE of *HSP70* in pretreated and challenged cells/RE of *HSP70* in challenged cells) × 100, where RE is relative expression.
[4] Percent (%) of production was calculated by [(HSP70 concentration/protein concentration in pretreated and challenged cells)/(HSP70 concentration/protein concentration in challenged cells)] × 100, where the concentration of HSP70 is ng/mL and the concentration of protein is μg/mL.

IL10 in BMDM whereas D-methionine and DL-methionine did not affect the production. Inclusion of methionine regardless of its types at 2500 mg/L reduced ($P < 0.05$) the production of ROS in IPEC-J2 and the effects of L-methionine was greater ($P < 0.05$) than D-methionine and DL-methionine on the production of ROS. Inclusion of L-methionine increased ($P < 0.05$) the production of *HSP70* in IPEC-J2 whereas D-methionine and DL-methionine did not affect the production of *HSP70*. Inclusion of L-methionine increased ($P < 0.05$) the production of *HSP70* in BMDM whereas D-methionine and DL-methionine reduced ($P < 0.05$) it.

4. Discussion

4.1. The GIT application

Measuring digestibility of feedstuffs using the multi-step porcine in vitro system provided reasonably controlled and uniform results with small variations among replications. The size of standard error was less than 1% of the digestibility of dry matter and crude protein, allowing the use only 3 replications to be sufficient to detect statistical differences at $P < 0.01$. Whereas, the size of standard errors when measuring digestibility from recently published papers using animal trials averaged 6.5% (Fig. 10), requiring a minimum of 8 to 12 replications to detect statistical differences at $P < 0.05$ (Cheng et al., 2021, 2022; Deng et al., 2023a,b; Duarte et al., 2021; Moita et al., 2022).

Supplementation of xylanase (4 XU/kg) increased ($P < 0.05$) dry matter digestibility of wheat by 4% and barley by 2% and standard errors were 0.1% and 0.3%, respectively, despite only 3 replicates were used. Moita et al. (2022) used the same source of xylanase in an animal experiment and demonstrated that apparent ileal digestibility (AID, %) of dry matter and crude protein was numerically increased by 6% and 7%, but it was not statistically different ($P = 0.102$ and $P = 0.058$, respectively) due to a relatively large standard error (3% of the mean) despite using 12 replicates.

Using the multi-step porcine in vitro system in the current study, supplementation of xylanase (4 XU/kg) reduced ($P < 0.05$) digesta viscosity of wheat by 21% and barley by 10% and the standard errors were 1.3% and 0.7% of the viscosity for wheat and barley, respectively, with the use of 3 replicates. Moita et al. (2022) also showed that the use of the same source of xylanase reduced ($P < 0.05$) digesta viscosity by 17% and the standard error was 7% of the mean using 12 replicates in the in vivo porcine model. Similarly, other in vivo studies showed a reduction of digesta viscosity with the use of xylanase (Duarte et al., 2020; Passos et al., 2015; Tiwari

Table 7
Viability of intestinal porcine epithelial cells (IPEC-J2) with different dose levels of tryptophan (Trp, %).

Item	Trp, mg/L										SEM	*P*-value		
	0	10	20	39	78	156	313	625	1250	2500		Linear	Quadratic	0 vs. Trp
Viability[1]	100.0	96.0	97.0	107.2	100.4	89.3	75.0	64.1	42.0	22.3	5.67	<0.001	0.001	<0.001

[1] Cell viability (%) was calculated by (OD_{450} of treated cells/OD_{450} of untreated cells) × 100, where OD_{450} is an optical density at 450 nm.

Table 8
Reduction of *IL8*, IL10, and ROS, and production of HSP70 and cell proliferation in IPEC-J2 and BMDM with increasing dose levels of tryptophan from 0 to 100 mg/L.

Item	Cell type	Tryptophan, mg/L			SEM	*P*-value	
		0	50	100		Linear	Quadratic
IL8, % reduction[1]	IPEC-J2	0.0	7.5	−0.5	3.23	0.914	0.048
IL10, pg/mL	BMDM	0.0	47.8	133.1	9.51	<0.001	0.195
ROS, % reduction[2]	IPEC-J2	0.0	14.3	20.5	1.64	<0.001	0.065
HSP70, % production[3]	IPEC-J2	100.0	110.2	222.0	9.75	<0.001	0.001
HSP70, % production[4]	BMDM	100.0	162.6	223.9	13.17	<0.001	0.973
Proliferation, % increase[5]	IPEC-J2	100.0	109.5	114.7	1.63	<0.001	0.311

IL8 = interleukin 8; IL10 = interleukin 10; ROS = reactive oxygen species; HSP70 = heat shock protein 70; IPEC-J2 = intestinal porcine epithelial cells; BMDM = bone marrow-derived macrophages.
[1] Percent (%) of reduction was calculated by [(RGE of challenged cells − RGE of pretreated and challenged cells)/RGE of challenged cells] × 100, where RGE is relative gene expression.
[2] Percent (%) of reduction was calculated by [(RFU of challenged cells − RFU of pretreated and challenged cells)/RFU of challenged cells] × 100, where RFU is relative fluorescence units.
[3] Percent (%) of production was calculated by (RE of *HSP70* in pretreated and challenged cells/RE of *HSP70* in challenged cells) × 100, where RE is relative expression.
[4] Percent (%) of production was calculated by [(HSP70 concentration/protein concentration in pretreated and challenged cells)/(HSP70 concentration/protein concentration in challenged cells)] × 100, where the concentration of HSP70 is ng/mL and the concentration of protein is μg/mL.
[5] Percent (%) of increase was calculated by (OD_{450} of pretreated cells/OD_{450} of untreated cells) × 100, where OD_{450} is optical density at 450 nm.

Table 9
Viability of intestinal porcine epithelial cells (IPEC-J2) with different dose levels of methionine (Met, %).

Viability[1]	Met, mg/L							SEM	*P*-value		
	0	156.3	312.5	625	1250	2500	5000		Linear	Quadratic	0 vs. Met
L-Met	100.0	108.4	110.2	109.9	109.3	102.8	86.5	3.57	0.001	0.019	0.507
DL-Met	100.0	125.0	125.4	123.5	124.7	116.5	102.6	4.97	0.024	0.019	0.004
D-Met	100.0	110.9	113.1	116.6	108.9	105.7	103.6	9.34	0.591	0.744	0.293
All	100.0	111.9	113.6	113.3	112.4	105.8	91.4	2.78	<0.001	0.003	0.062

[1] Cell viability (%) was calculated by (OD_{450} of treated cells/OD_{450} of untreated cells) × 100, where OD_{450} is an optical density at 450 nm.

Table 10
Reduction of *IL8*, IL10, and ROS, and production of HSP70 in IPEC-J2 and BMDM with various methionine (Met) sources (DL-Met, D-Met, and L-Met).

Item	Cell type	Met, mg/L				SEM	*P*-value
		0	2500 (DL-Met)	2500 (D-Met)	2500 (L-Met)		
IL8, % reduction[1]	IPEC-J2	0.0[a]	18.4[b]	12.4[ab]	28.5[c]	2.77	<0.001
IL10, pg/mL	BMDM	0.0[a]	0.0[a]	0.0[a]	81.4[b]	13.04	<0.001
ROS, % reduction[2]	IPEC-J2	0.0[a]	7.36[a]	10.1[a]	19.3[b]	4.01	<0.001
HSP70, % production[3]	IPEC-J2	100.0[a]	100.8[a]	105.8[a]	247.3[b]	28.22	<0.001
HSP70, % production[4]	BMDM	100.0[a]	96.7[a]	97.4[ab]	156.8[b]	20.80	0.019

IL8 = interleukin 8; IL10 = interleukin 10; ROS = reactive oxygen species; HSP70 = heat shock protein 70; IPEC-J2 = intestinal porcine epithelial cells; BMDM = bone marrow-derived macrophages.
[a–c]Means within a row lacking common superscripts differ ($P < 0.05$).
[1] Percent (%) of reduction was calculated by [(RGE of challenged cells − RGE of pretreated and challenged cells)/RGE of challenged cells] × 100, where RGE is relative gene expression.
[2] Percent (%) of reduction was calculated by [(RFU of challenged cells − RFU of pretreated and challenged cells)/RFU of challenged cells] × 100, where RFU is relative fluorescence units.
[3] Percent (%) of production was calculated by (RE of *HSP70* in pretreated and challenged cells/RE of *HSP70* in challenged cells) × 100, where RE is relative expression.
[4] Percent (%) of production was calculated by [(HSP70 concentration/protein concentration in pretreated and challenged cells)/(HSP70 concentration/protein concentration in challenged cells)] × 100, where the concentration of HSP70 is ng/mL and the concentration of protein is μg/mL.

et al., 2018) requiring 12 to 16 replicates per treatment to detect statistical differences.

Our results demonstrate that, in vitro systems, if controlled properly, yield statistically valid results even with a small number of replicates compared with in vivo studies. It is interesting to observe that the magnitude of xylanase effects on digestibility and viscosity was similar between our in vitro results and in vivo studies published in the literature, validating the reliability and practical relevance of the multi-step porcine in vitro system.

Digestion of corn, corn DDGS, and soybean meal with xylanase yielded increased amount of XOS with xylotriose being the dominant oligosaccharide (Fig. 7), whereas wheat and barley had xylobiose, xylotriose, and xylotetraose. According to a review by Baker et al. (2021), the amounts of xylans in corn, soybean meal, corn DDGS, wheat, and barley are 17, 62, 17, 29, and 24 mg/kg, respectively. In this study, the amount of XOS generated from these feedstuffs were 0.6, 0.5, 1.1, 15.5, and 11.2 mg/kg for corn, soybean meal, corn DDGS, wheat, and barley, respectively, indicating that 4%, 3%, 2%, 53%, and 47% of xylans, respectively, were hydrolyzed by xylanase. Production of XOS from xylan hydrolysis is biologically important for their physicochemical and prebiotic effects enhancing intestinal health of animals (Chen et al., 2020; Finegold et al., 2014; Okazaki et al., 1990). In this study, the multi-step porcine in vitro system closely mimicked in vivo experiments in demonstrating the functional role of xylanase supplemented in various feedstuffs (Moita and Kim, 2022).

The use of phytase (200 FTU/mL) in the multi-step porcine in vitro system showed a rapid increase ($P < 0.05$) of phosphorus

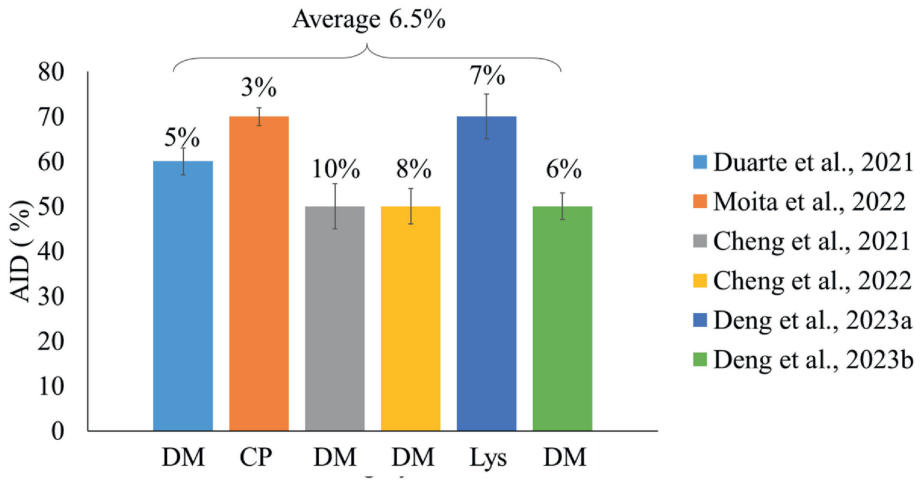

Fig. 10. Apparent ileal digestibility (AID) of dry matter (DM), crude protein (CP), and lysine (Lys) in diets fed to pigs and the standard error values of digestibility coefficients from each study (Cheng et al., 2021, 2022; Duarte et al., 2021; Moita et al., 2022; Deng et al., 2023a,b).

release, up to 31% from phytic acid during 360-min digestion using 3 replicates. An in vivo study using 12 replicates for each 5 levels of the same bacterial 6-phytase used in this study showed a linear increase of AID phosphorus from 79% to 85% with up to 5000 FTU/kg feed in nursery pigs (Moita and Kim, 2023). Similarly, other in vivo studies showed an increase of phosphorus digestibility with the use of phytase (Kies et al., 2006; Lee et al., 2017; Lu et al., 2020) requiring 8 to 14 replicates per treatment.

Several multi-step in vitro digestion systems have been evaluated and shown to successfully simulate nutrient digestibility and digestion in pigs (Egger et al., 2017; Graham et al., 1989; Jha and Zijlstra, 2019; Regmi et al., 2009). Advances in control technology and sensors allow extended automations of in vitro systems with improved precision and repeatability. Differently from previous in vitro digestion evaluations, this study used only 3 replications based on pre-tests done internally. In biological research and in general science, the minimal number of experimental replication is 3 for valid statistical evaluations (Botella et al., 2006; Fitts, 2011; Maxwell et al., 2008). With the use of 3 replications in this multi-step porcine in vitro system, differences between or among treatments were statistically detected at $P < 0.05$ with the size of standard errors less than 1% of treatment means. The 12 digestion chambers used in this in vitro system had a fully automated control of injection pumps, cooling, heating, and stirring that were monitored during the digestion process. This automation successfully enhanced repeatability of the results and consistency among 12 digestion chambers. Enhanced repeatability and precision add additional values to existing advantages of the in vitro digestion systems including reduced research cost, reduced research duration, and increased applicability compared to in vivo studies (Vinyard and Faciola, 2022).

4.2. The Cell application

For the evaluation of the role of additives on immunological reactions to intestinal epithelial cells (IPEC-J2) and immune cells (BMDM), the Cell Application of the multi-step porcine in vitro system was developed and tested. For this test, arginine, tryptophan, and methionine were selected as additives for their functional roles to intestinal epithelial cells and immune cells. These amino acids are often classified as “functional amino acids” for their unique roles in an animal body in addition to their traditional roles in protein synthesis (Kim et al., 2006, 2019; Wu and Kim, 2007).

Prior to Cell application of arginine, tryptophan, and methionine, their impacts on cell viability were tested. For non-clinical risk assessment of substances (such as feed supplements), there is an agreed term called “no observed adverse effect level (NOAEL)”. The US FDA defines the NOAEL as “the maximum inclusion level of a substance without a significant increase in adverse effects in comparison to the control group” (FDA, 2005). There are research findings that show the NOAEL for supplemental amino acids fed to pigs. The NOAEL of arginine, tryptophan, and methionine are evaluated to be 2% (Hu et al., 2015), 1% (Chung et al., 1991), and 1% (Edmonds and Baker, 1987), respectively, in feeds fed to pigs. In the current in vitro cell culture model, viability of IPEC-J2 was not affected until 2502 mg/L arginine, 1006 mg/L tryptophan, and 2510 mg/L methionine were added. These values provide references to how much each amino acid could be supplemented in subsequent in vitro cell culture models to evaluate their effects on inflammatory, oxidative stress, and heat stress statuses.

Arginine has one of the most versatile roles in an animal body among amino acids. Functional roles of arginine in pigs are extensively investigated and reviewed (Kim et al., 2006; Wu et al., 2004, 2007) including its vasodilatory (Kim et al., 2010; Zhan et al., 2008), angiogenic (Zhan et al., 2008), anti-inflammatory (Liu et al., 2008; Zhan et al., 2008), anti-oxidative (Bergeron and Guay, 2019; Ma et al., 2010), anabolic (Kim and Wu, 2004), and anti-heat stress (Wu et al., 2010) properties. Using the multi-step porcine in vitro system, this study demonstrated that arginine reduced inflammatory response and oxidative stress in IPEC-J2. Liu et al. (2008) evaluated the anti-inflammatory effects of arginine fed to nursery pigs and showed a 50% reduction in tumor necrosis factor alpha (TNF-α) and a 41% reduction of IL6 in the jejunal mucosa and Bergeron and Guay (2019) showed an 11% reduction in malondialdehyde. Ma et al. (2010) showed a 32% reduction in hydroxyl radical, a 15% increase in glutathione, and a 27% increase in total antioxidative capacity in pigs fed diets with arginine supplementation up to 1%. The results from in vivo studies show similar anti-inflammatory and anti-oxidative effects of arginine observed in this in vitro study. These functional benefits of arginine may relate to enhanced efficiency in pig production (Kim and Wu, 2004; Mateo et al., 2007, 2008).

Tryptophan is an essential amino acid for the growth of animals but it also possesses specific functions in the body as the precursor of serotonin, melatonin, 3-OH-kynurenine, and indole (Kim et al., 2006, 2019; Sève, 1999). These metabolites from tryptophan are

shown to have anti-inflammatory (Le Floc'h et al., 2008; Qiu et al., 2011; Shen et al., 2021), anti-oxidative (Mao et al., 2014; Shen et al., 2012a), and anti-stress (Koopmans et al., 2006; Shen et al., 2012b) properties in pigs. Using the multi-step porcine in vitro system, this study demonstrated that tryptophan reduced inflammatory response both in IPEC-J2 and BMDM, reduced oxidative stress in IPEC-J2, increased the production of *HSP70* in both IPEC-J2 and BMDM, and increased the proliferation of IPEC-J2, agreeing with the previous findings with pigs. Le Floc'h et al. (2008) showed a 175% increase of haptoglobin in the serum of pigs fed a diet with 0.55% tryptophan supplementation and Mao et al. (2014) showed a 31% increase of glutathione in the liver of pigs fed a diet with 0.45% tryptophan supplementation indicating anti-inflammatory and anti-oxidative functions of tryptophan when supplemented above the nutritional requirement. These in vivo results concur with the current in vitro findings. These functional benefits of tryptophan are shown to enhance efficiency of pig production (Le Floc'h and Sève, 2007; Shen et al., 2015a; Trevisi et al., 2009)

Methionine is another critically important essential amino acid for the growth of animals. In addition to its primary role in protein synthesis, methionine also possesses specific functions in the body as the precursor of glutathione, taurine, polyamines, and others possessing anti-oxidative property (Brosnan et al., 2007; Park et al., 2018; Shen et al., 2014) and functions as a methyl donor (Finkelstein, 1990; Kim et al., 2019; Reddy et al., 1994). Using the multi-step porcine in vitro system, the current study showed that L-methionine and DL-methionine were effective in reducing inflammatory status and oxidative stress status whereas D-methionine was not effective. Shen et al. (2014) showed in the in vivo study that L-methionine effectively reduced oxidative damages in the small intestine of nursery pigs compared with DL-methionine. Similar results were obtained in broiler chickens (Shen et al., 2015b) and turkey poults (Park et al., 2018). Considering that only L-methionine is biologically functional whereas D-methionine needs to be converted to L-methionine, requiring D-amino acid oxidase and transaminase (Hasegawa et al., 2005; Saunderson, 1985), no effects of D-methionine was expected in this vitro cell culture because the culture media did not include D-amino acid oxidase and transaminase. This in vitro cell culture model clearly showed anti-oxidative properties of L-methionine similar to in vivo studies when comparing it with D-methionine (Chen et al., 2014; Shen et al., 2014). However, in vivo studies from Espinosa et al. (2021), Htoo and Morales (2016), and Tian et al. (2016) showed indifferent effects between L-methionine and D-methionine. Different outcomes of the efficacy or biological effects of L-methionine vs. D-methionine among in vivo studies could possibly due to the degree of impacts of methionine sources related to their supplementation levels, and difference in age of pigs because their ability expressing oxidase and transaminase in the liver and kidney would be different. The use of the in vitro cell culture model in the evaluation of methionine sources allowed the control of the specific conditions, such as complication of enzyme availability, whereas there are limitations as to how much can be controlled when running an animal experiment despite the best effort.

5. Conclusion

Nutrient digestibility and the effects of feed additives on anti-inflammatory, anti-oxidative, and anti-heat stress statuses could be evaluated using the multi-step porcine in vitro system with electronic control and automation. The use of this in vitro model allowed the use of minimal number of experimental replications without compromising statistical validity. Recent advances in control technology and sensors improve precision and consistency of in vitro research models, leading to their increased uptake for nutrition research in lieu of costly animal studies.

Author contributions

Sung Woo Kim: Conceptualization, Methodology, Validation, Resources, Writing – Original Draft, Visualization, Writing – Review & Editing, Supervision, Project administration, Funding acquisition. **Hee Yeon Kim:** Methodology, Formal analysis, Investigation, Validation, Data Curation, Writing – Review & Editing, Visualization. **Jun-Ok Moon:** Conceptualization, Methodology, Investigation, Formal analysis, Investigation, Data Curation, Writing – Review & Editing, Visualization.

Declaration of competing interest

The research system used (in vitro system) belongs to CJ Blossom Park. Two co-authors (Hee Yeon Kim and Jun-OK Moon) are currently employed by CJ Blossom Park as research scientists. CJ BIO and CJ Blossom Park are financially independent and no financial interests.

Acknowledgments

The authors thank technical supports from all members of the Application Center at the CJ Blossom Park (Suwon, Republic of Korea) and Kim Lab at North Carolina State University (Raleigh, NC, USA) and financial supports from North Carolina Agricultural Foundation (Raleigh, NC, USA) and CJ BIO (Seoul, Republic of Korea).

References

Adur MK, Seibert JT, Romoser MR, Bidne K, Baumgard LH, Keating AF, et al. Porcine endometrial heat shock proteins are differentially influenced by pregnancy status, heat stress, and altrenogest supplementation during the peri-implantation period. J Anim Sci 2022;100(7):skac129. https://doi.org/10.1093/jas/skac129.

AOAC. Official methods of analysis. 18th ed. Gaithersburg, MD: AOAC International; 2007.

ASAS. ASAS midwest section meeting abstracts. J Anim Sci 2022a;100(Suppl. 2):1–206 [Abstract].

ASAS. ASAS annual 2022 meeting abstracts. J Anim Sci 2022b;100(Suppl. 3):1–406.

Ayres VE, Broomhead JN, Li X, Raab RM, Moritz JS. Viscosity and growth response of broilers fed high fiber diets supplemented with a corn-produced recombinant carbohydrase. J Appl Poult 2019;28(4):826–36. https://doi.org/10.3382/japr/pfz039.

Baker JT, Duarte ME, Holanda DM, Kim SW. Friend or Foe? Impacts of dietary xylans, xylooligosaccharides, and xylanases on intestinal health and growth performance of monogastric animals. Animals 2021;11:609. https://doi.org/10.3390/ani11030609.

Bedford MR, Classen HL. An in vitro assay for prediction of broiler intestinal viscosity and growth when fed rye-based diets in the presence of exogenous enzymes. Poult Sci 1993;72:137–43. https://doi.org/10.3382/ps.0720137.

Bergeron N, Guay F. Impact of zinc and arginine on antioxidant status of weanling piglets raised under commercial conditions. Amin Nutr 2019;5:227–33. https://doi.org/10.1016/j.aninu.2019.03.001.

Biancarosa I, Espe M, Bruckner CG, Heesch S, Liland N, Waabø R, et al. Amino acid composition, protein content, and nitrogen-to-protein conversion factors of 21 seaweed species from Norwegian waters. J Appl Phycol 2017;29:1001–9. https://doi.org/10.1007/s10811-016-0984-3.

Bodas R, López S, Fernández M, García-González R, Rodríguez AB, Wallace RJ, et al. In vitro screening of the potential of numerous plant species as anti-methanogenic feed additives for ruminants. Anim Feed Sci Technol 2008;145:245–58. https://doi.org/10.1016/j.anifeedsci.2007.04.015.

Boisen S, Fernández JA. Prediction of the apparent ileal digestibility of protein and amino acids in feedstuffs and feed mixtures for pigs by in vitro analyses. Anim Feed Sci Technol 1995;51:29–43. https://doi.org/10.1016/0377-8401(94)00686-4.

Boisen S, Fernández JA. Prediction of the total tract digestibility of energy in feedstuffs and pig diets by in vitro analyses. Anim Feed Sci Technol 1997;68:277–86. https://doi.org/10.1016/S0377-8401(97)00058-8.

Botella J, Ximenez C, Revuelta J, Suero M. Optimization of sample size in controlled experiments: the CLAST rule. Behav Res Methods 2006;38:65–76. https://doi.org/10.3758/bf03192751.

Bouffi C, Wikenheiser-Brokamp KA, Chaturvedi P, Sundaram N, Goddard GR, Wunderlich M, et al. In vivo development of immune tissue in human intestinal organoids transplanted into humanized mice. Nat Biotechnol 2023;41(6):824–31. https://doi.org/10.1038/s41587-022-01558-x.

Brosnan JT, Brosnan ME, Bertolo RF, Brunton JA. Methionine: a metabolically unique amino acid. Livest Sci 2007;112:2–7. https://doi.org/10.1016/j.livsci.2007.07.005.

Bryan DDSL, Abbott DA, Classen HL. Development of an in vitro protein digestibility assay mimicking the chicken digestive tract. Anim Nutr 2018;4(4):401–9. https://doi.org/10.1016/j.aninu.2018.04.007.

Chen H, Zhang S, Kim SW. Effects of supplemental xylanase on gut health and growth performance of nursery pigs fed diets with corn distillers' dried grains with solubles. J Anim Sci 2020;98. https://doi.org/10.1093/jas/skaa185. skaa185.

Chen WLK, Edington C, Suter E, Yu J, Velazquez JJ, Velazquez JG, et al. Integrated gut/liver microphysiological systems elucidates inflammatory inter-tissue crosstalk. Biotechnol Bioeng 2017;114(11):2648–59. https://doi.org/10.1002/bit.26370.

Chen Y, Li D, Dai Z, Piao X, Wu Z, Wang B, et al. L-Methionine supplementation maintains the integrity and barrier function of the small-intestinal mucosa in post-weaning piglets. Amino Acids 2014;46:1131–42. https://doi.org/10.1007/s00726-014-1675-5.

Cheng YC, Duarte ME, Kim SW. Functional and nutritional values of lysed *Corynebacterium glutamicum* cell mass for gut health and growth of newly weaned pigs. J Anim Sci 2021;99:skab331. https://doi.org/10.1093/jas/skab331.

Cheng YC, Duarte ME, Kim SW. Effects of Yarrowia lipolytica supplementation on growth performance, intestinal health and apparent ileal digestibility of diets fed to nursery pigs. Anim Biosci 2022;35:605–13. https://doi.org/10.5713/ab.21.0369.

Cheryl LD, George CF. Viscosity as related to dietary fiber: a review. Crit Rev Food Sci Nutr 2006;46(8):649–63. https://doi.org/10.1080/10408390500511862.

Cheryl LD, Michael RM, George CF. Dietary fibers affect viscosity of solutions and simulated human gastric and small intestinal digesta. J Nutr 2006;136:913–9. https://doi.org/10.1093/jn/136.4.913.

Choi H, Won CS, Kim BG. Protein and energy concentrations of meat meal and meat and bone meal fed to pigs based on in vitro assays. Anim Nutr 2021;7:252–7. https://doi.org/10.1016/j.aninu.2020.07.007.

Choi H, Chen Y, Longo F, Kim SW. Comparative effects of benzoic acid and sodium benzoate in diets for nursery pigs on growth performance and acidification of digesta and urine. J Anim Sci 2023;101:skad116. https://doi.org/10.1093/jas/skad116.

Chung TK, Gelberg HB, Dorner JL, Baker DH. Safety of L-tryptophan for pigs. J Anim Sci 1991;69(7):2955–60. https://doi.org/10.2527/1991.6972955x.

Cui YJ, Chen LY, Zhou X, Tang ZN, Wang C, Wang HF. Heat stress induced IPEC-J2 cells barrier dysfunction through endoplasmic reticulum stress mediated apoptosis by p-eif2α/CHOP pathway. J Cell Physiol 2022;237(2):1389–405. https://doi.org/10.1002/jcp.30603.

De Leoz ML, Wu S, Strum JS, Niñonuevo MR, Gaerlan SC, Mirmiran M, et al. A quantitative and comprehensive method to analyze human milk oligosaccharide structures in the urine and feces of infants. Anal Bioanal Chem 2013;405(12):4089–105. https://doi.org/10.1007/s00216-013-6817-1.

Deng Z, Duarte ME, Jang KB, Kim SW. Soy protein concentrate replacing animal protein supplements and its impacts on intestinal health, mucosa-associated microbiota, and growth performance of nursery pigs. J Anim Sci 2022;100:skac255. https://doi.org/10.1093/jas/skac255.

Deng Z, Duarte ME, Kim SW. Efficacy of soy protein concentrate replacing animal protein supplements in mucosa-associated microbiota, intestinal health, and growth performance of nursery pigs. Anim Nutr 2023a;14:235–48. https://doi.org/10.1016/j.aninu.2023.06.007.

Deng Z, Duarte ME, Kim SY, Hwang Y, Kim SW. Comparative effects of soy protein concentrate, enzyme-treated soybean meal, and fermented soybean meal replacing animal protein supplements in feeds on growth performance and intestinal health of nursery pigs. J Anim Sci Biotechnol 2023b;14:89. https://doi.org/10.1186/s40104-023-00888-3.

Duarte ME, Kim SW. Intestinal microbiota and its interaction to intestinal health in nursery pigs. Anim Nutr 2022;8:169–84. https://doi.org/10.1016/j.aninu.2021.05.001.

Duarte ME, Zhou F, Dutra W, Kim SW. Dietary supplementation of xylanase and protease on performance, digesta viscosity, nutrient digestibility, immune and oxidative stress status and gut health of newly weaned pigs. Anim Nutr 2019;5:351–8. https://doi.org/10.1016/j.aninu.2019.04.005.

Duarte ME, Tyus J, Kim SW. Synbiotic effects of enzyme and probiotics on intestinal health and growth of newly weaned pigs challenged with enterotoxigenic F18+ *Escherichia coli*. Front Vet Sci 2020;7:573. https://doi.org/10.3389/fvets.2020.00573.

Duarte ME, Sparks C, Kim SW. Modulation of jejunal mucosa-associated microbiota in relation to intestinal health and nutrient digestibility in pigs by supplementation of β-glucanase to corn–soybean meal-based diets with xylanase. J Anim Sci 2021;99:skab190. https://doi.org/10.1093/jas/skab190.

Durmic Z, Moate PJ, Eckard R, Revell DK, Williams R, Vercoe PE. In vitro screening of selected feed additives, plant essential oils and plant extracts for rumen methane mitigation. J Sci Food Agric 2014;94:1191–6. https://doi.org/10.1002/jsfa.6396.

Edmonds MS, Baker DH. Amino acid excesses for young pigs: effects of excess methionine, tryptophan, threonine or leucine. J Anim Sci 1987;64(6):1664–71. https://doi.org/10.2527/jas1987.6461664x.

Egger L, Schlegel P, Baumann C, Stoffers H, Guggisberg D, Brügger C, et al. Physiological comparability of the harmonized INFOGEST in vitro digestion method to in vivo pig digestion. Food Res Int 2017;102:567–74. https://doi.org/10.1016/j.foodres.2017.09.047.

Espinosa CD, Mathi JK, Blavi L, Liu Y, Htoo JK, Gonzales-Vega CJ, et al. Effects of supplemental D-methionine in comparison to L-methionine on nitrogen retention, gut morphology, antioxidant status, and mRNA abundance of amino acid transporters in weanling pigs. J Anim Sci 2021;99:skab248. https://doi.org/10.1093/jas/skab248.

Finegold SM, Li Z, Summanen PH, Downes J, Thames G, Corbett K, et al. Xylooligosaccharide increases bifidobacteria but not lactobacilli in human gut microbiota. Food Funct 2014;5:436–45. https://doi.org/10.1039/C3FO60348B.

Fitts DA. Ethics and animal numbers: informal analyses, uncertain sample sizes, inefficient replications, and type I errors. J Am Assoc Lab Anim Sci 2011;50:445–53.

Folch J, Lees M, Sloane Stanley GH. A simple method for the isolation and purification of total lipides from animal tissues. J Biol Chem 1957;226(1):497–509. https://doi.org/10.1016/S0021-9258(18)64849-5.

Food and Drug Administration (FDA). Center for Drug Evaluation and Research (CDER), US Department of Health and Human Services. Guidance for industry: estimating the maximum safe starting dose in initial clinical trials for therapeutics in adult healthy volunteers. 2005.

Finkelstein JD. Methionine metabolism in mammals. J Nutr Biochem 1990;1:228–37. https://doi.org/10.1016/0955-2863(90)90070-2.

Gao J, Scheenstra MR, van Dijk A, Veldhuizen EJA, Haagsman HP. A new and efficient culture method for porcine bone marrow-derived M1- and M2-polarized macrophages. Vet Immunol Immunopathol 2018;200:7–15. https://doi.org/10.1016/j.vetimm.2018.04.002.

Graham H, Löwgren W, Åman P. An in vitro method for studying digestion in the pig: 2. Comparison with in vivo ileal and faecal digestibilities. Br J Nutr 1989;61:689–98. https://doi.org/10.1079/BJN19890155.

Greiner R. Limitations of an in vitro model of the poultry digestive tract on the evaluation of the catalytic performance of phytases. J Sci Food Agric 2021;101(6):2519–24. https://doi.org/10.1002/jsfa.10878.

Hasegawa H, Shinohara Y, Akahane K, Hashimoto T. Direct detection and evaluation of conversion of d-methionine into l-methionine in rats by stable isotope methodology. J Nutr 2005;135:2001–5. https://doi.org/10.1093/jn/135.8.2001.

Hirvonen J, Liljavirta J, Saarinen MT, Lehtinen MJ, Ahonen I, Nurminen P. Effect of phytase on in vitro hydrolysis of phytate and the formation of myo-inositol phosphate esters in various feed materials. J Agric Food Chem 2019;67(41):11396–402. https://doi.org/10.1021/acs.jafc.9b03919.

Htoo JK, Morales J. Bioavailability of L-methionine relative to DL-methionine as a methionine source for weanling pigs. J Anim Sci 2016;94:249–52. https://doi.org/10.2527/jas.2015–9796.

Hu S, Li X, Rezaei R, Meininger CJ, McNeal CJ, Wu G. Safety of long-term dietary supplementation with L-arginine in pigs. Amino Acids 2015;47(5):925–36. https://doi.org/10.1007/s00726-015-1921-5.

Jang KB, Purvis JM, Kim SW. Dose–response and functional role of whey permeate as a source of lactose and milk oligosaccharides on intestinal health and growth of nursery pigs. J Anim Sci 2021;99:skab008. https://doi.org/10.1093/jas/skab008.

Jang KB, Kim SW. Role of milk carbohydrates in intestinal health of nursery pigs: a review. J Anim Sci Biotechnol 2022;13:1–14. https://doi.org/10.1186/s40104-021-00650-7.

Jang KB, Moita VHC, Martinez N, Sokale A, Kim SW. Efficacy of zinc glycinate reducing zinc oxide on intestinal health and growth of nursery pigs challenged with F18+ *Escherichia coli*. J Anim Sci 2023;101:skad035. https://doi.org/10.1093/jas/skad035.

Jean N, Yolande JP. Prediction of digestibility of organic matter and energy in the growing pig from an in vitro method. Anim Feed Sci Technol 2007;134(3):211–22. https://doi.org/10.1016/j.anifeedsci.2006.07.008.

Jeong JY, Kwon SG, Hwang JH, Park DH, Bang WY, Kim TW, et al. Differential expressions of HSP27 and HSP70 is induced in thelongissimus dorsimuscle of fattening pigs fed a fermented carrot by-product. J Appl Anim Res 2014;42(3):321–6. https://doi.org/10.1080/09712119.2013.867859.

Jha R, Kim SW. Editorial: nutritional intervention for the intestinal health of young monogastric animals. Front Vet Sci 2021;8:668563. https://doi.org/10.3389/fvets.2021.668563.

Jha R, Zijlstra RT. Physico-chemical properties of purified starch affect their in vitro fermentation characteristics and are linked to in vivo fermentation characteristics in pigs. Anim Feed Sci Technol 2019;253:74–80. https://doi.org/10.1016/j.anifeedsci.2019.05.006.

Jin XC, Peng DQ, Kim SJ, Kim NY, Nejad JG, Kim D, et al. Vitamin A supplementation downregulates ADH1C and ALDH1A1 mRNA expression in weaned beef calves. Anim Nutr 2022;10:372–81. https://doi.org/10.1016/j.aninu.2022.06.007.

Kern M, Günzel D, Aschenbach JR, Tedin K, Bondzio A, Lodemann U. Altered cytokine expression and barrier properties after in vitro infection of porcine epithelial cells with Enterotoxigenic *Escherichia coli* and probiotic *Enterococcus faecium*. Mediat Inflamm 2017;2017:2748192. https://doi.org/10.1155/2017/2748192.

Kies AK, Kemme PA, Šebek LBJ, van Diepen JTM, Jongbloed AW. Effect of graded doses and a high dose of microbial phytase on the digestibility of various minerals in weaner pigs. J Anim Sci 2006;84:1169–75. https://doi.org/10.2527/2006.8451169x.

Kim SW, Easter RA. Nutritional value of fish meals in the diet for young pigs. J Anim Sci 2001;79:1829–39. https://doi.org/10.2527/2001.7971829x.
Kim SW, Duarte ME. Understanding intestinal health in nursery pigs and the relevant nutritional strategies. Anim Biosci 2021;34:338–44. https://doi.org/10.5713/ab.21.0010.
Kim SW, Wu G. Dietary arginine supplementation enhances the growth of milk-fed young pigs. J Nutr 2004;134:625–30. https://doi.org/10.1093/jn/134.3.625.
Kim SW, Mateo RD, Yin YL, Wu G. Functional amino acids and fatty acids for enhancing production performance of sows and piglets. Asian Australas J Anim Sci 2006;20:295–306. https://doi.org/10.5713/ajas.2007.295.
Kim SW, Perret-Gentil MI, Hart MW. Pyloric infusion of arginine increases portal vein blood flow in growing pigs. J Dairy Sci 2010;93:87–8.
Kim SW, Chen H, Parnsen W. Regulatory role of amino acids in pigs fed on protein-restricted diets. Curr Protein Pept Sci 2019;20:132–8. https://doi.org/10.2174/1389203719666180517100746.
Kitson RE, Mellon MG. Colorimetric determination of phosphorus as molybdivanadophosphoric acid. Ind Eng Chem Anal Ed 1944;16(6):379–83. https://doi.org/10.1021/i560130a017.
Koopmans SJ, Guzik AC, van der Meulen J, Dekker R, Kogut J, Kerr BJ, et al. Effects of supplemental L-tryptophan on serotonin, cortisol, intestinal integrity, and behavior in weanling piglets. J Anim Sci 2006;84:963–71. https://doi.org/10.2527/2006.844963x.
Kouzounis D, Sun P, Bakx EJ, Schols HA, Kabel MA. Strategy to identify reduced arabinoxylo-oligosaccharides by HILIC-MS. Carbohydr Polym 2022;289:119415. https://doi.org/10.1016/j.carbpol.2022.119415.
Lee JK, Duarte ME, Kim SW. 297 Super dosing effects of corn-expressed phytase on growth performance, bone characteristics, and nutrient digestibility in nursery pigs fed diets deficient in phosphorus and calcium. J Anim Sci 2017;95:144. https://doi.org/10.2527/asasmw.2017.297.
Le Floc'h N, Sève B. Biological roles of tryptophan and its metabolism: potential implications for pig feeding. Livest Sci 2007;112:23–32. https://doi.org/10.1016/j.livsci.2007.07.002.
Le Floc'h N, Melchoir D, Sève B. Dietary tryptophan helps to preserve tryptophan homeostasis in pigs suffering from lung inflammation. J Anim Sci 2008;86:3473–9. https://doi.org/10.2527/jas.2008-0999.
Li Y, Jiang X, Cai L, Zhang Y, Ding H, Yin J, et al. Effects of daidzein on antioxidant capacity in weaned pigs and IPEC-J2 cells. Anim Nutr 2022;11:48–59. https://doi.org/10.1016/j.aninu.2022.06.014.
Liu X, Quan N. Immune cell isolation from mouse femur bone marrow. Bio Protoc 2015;5(20):e1631. https://doi.org/10.21769/bioprotoc.1631.
Liu Y, Huang J, Hou Y, Zhu H, Zhao S, Ding B, et al. Dietary arginine supplementation alleviates intestinal mucosal disruption induced by Escherichia coli lipopolysaccharide in weaned pigs. Br J Nutr 2008;100:552–60. https://doi.org/10.1017/S0007114508911612.
Lock JY, Caboni M, Strandwitz P, Morrissette M, DiBona K, Joughin BA, et al. An in vitro intestinal model captures immunomodulatory properties of the microbiota in inflammation. Gut Microbes 2022;14(1):2039002. https://doi.org/10.1080/19490976.2022.2039002.
Lu H, Shin S, Kuehn I, Bedford M, Rodehutscord M, Adeola O, et al. Effect of phytase on nutrient digestibility and expression of intestinal tight junction and nutrient transporter genes in pigs. J Anim Sci 2020;98:skaa206. https://doi.org/10.1093/jas/skaa206.
Ma X, Lin Y, Jiang Z, Zheng C, Zhou G, Yu D, et al. Dietary arginine supplementation enhances antioxidative capacity and improves meat quality of finishing pigs. Amino Acids 2010;38:95–102. https://doi.org/10.1007/s00726-008-0213-8.
Mandalari G, Mackie AM, Rigby NM, Wickham MS, Mills EN. Physiological phosphatidylcholine protects bovine beta-lactoglobulin from simulated gastrointestinal proteolysis. Mol Nutr Food Res 2009;53:S131–9. https://doi.org/10.1002/mnfr.200800321.
Manfredi AP, Perotti NI, Martínez MA. Cellulose degrading bacteria isolated from industrial samples and the gut of native insects from Northwest of Argentina. J Basic Microbiol 2015;55(12):1384–93. https://doi.org/10.1002/jobm.201500269.
Mao X, Lv M, Yu B, He J, Zheng P, Yu J, et al. The effect of dietary tryptophan levels on oxidative stress of liver induced by diquat in weaned piglets. J Anim Sci Biotechnol 2014;5:49. https://doi.org/10.1186/2049-1891-5-49.
Mateo RD, Wu G, Bazer FW, Park JC, Shinzato I, Kim SW. Dietary L-arginine supplementation enhances the reproductive performance of gilts. J Nutr 2007;137:652–6. https://doi.org/10.1093/jn/137.3.652.
Mateo RD, Wu G, Moon HK, Carroll JA, Kim SW. Effects of dietary arginine supplementation during gestation and lactation on the performance of lactating primiparous sows and nursing piglets. J Anim Sci 2008;86:827–35. https://doi.org/10.2527/jas.2007-0371.
Marco A, Rubio R, Compano R, Casals I. Comparison of the Kjeldahl method and a combustion method for total nitrogen determination in animal feed. Talanta 2002;57(5):1019–26. https://doi.org/10.1016/S0039-9140(02)00136-4.
Maxwell SE, Kelley K, Rausch JR. Sample size planning for statistical power and accuracy in parameter estimation. Annu Rev Psychol 2008;59:537–63. https://doi.org/10.1146/annurev.psych.59.103006.093735.
McCracken BA, Spurlock ME, Roos MA, Zuckermann FA, Gaskins HR. Weaning anorexia may contribute to local inflammation in the piglet small intestine. J Nutr 1999;129:613–9. https://doi.org/10.1093/jn/129.3.613.
Moita VHC, Kim SW. Nutritional and functional roles of phytase and xylanase enhancing the intestinal health and growth of nursery pigs and broiler chickens. Animals 2022;12:3322. https://doi.org/10.3390/ani12233322.
Moita VHC, Kim SW. Efficacy of a bacterial 6-phytase supplemented beyond traditional dose levels on jejunal mucosa-associated microbiota, ileal nutrient digestibility, bone parameters, and intestinal health, and growth performance of nursery pigs. J Anim Sci 2023;101:skad134. https://doi.org/10.1093/jas/skad134.
Moita VHC, Duarte ME, da Silva SN, Kim SW. Supplemental effects of functional oils on the modulation of mucosa-associated microbiota, intestinal health, and growth performance of nursery pigs. Animals 2021a;11:1591. https://doi.org/10.3390/ani11061591.
Moita VHC, Duarte ME, Kim SW. Supplemental effects of phytase on modulation of mucosa-associated microbiota in the jejunum and the impacts on nutrient digestibility, intestinal morphology, and bone parameters in broiler chickens. Animals 2021b;11:3351. https://doi.org/10.3390/ani11123351.
Moita VHC, Duarte ME, Kim SW. Functional roles of xylanase enhancing intestinal health and growth performance of nursery pigs by reducing the digesta viscosity and modulating the mucosa-associated microbiota in the jejunum. J Anim Sci 2022;100:skac116. https://doi.org/10.1093/jas/skac116.
Na YR, Jung D, Gu GJ, Seok SH. GM-CSF grown bone marrow derived cells are composed of phenotypically different dendritic cells and macrophages. Mol Cells 2016;39(10):734–41. https://doi.org/10.14348/molcells.2016.0160.
Okazaki M, Fujikawa S, Matsumoto N. Effect of xylooligosaccharide on the growth of Bifidobacteria. Bifid Microflora 1990;9:77–86. https://doi.org/10.12938/bifidus1982.9.2_77.
Park I, Pasquetti T, Malheiros RD, Ferket PR, Kim SW. Effects of supplemental L-methionine on growth performance and redox status of Turkey poults compared with the use of DL-methionine. Poult Sci 2018;97:102–9. https://doi.org/10.3382/ps/pex259.
Parra MC, Forwood DL, Chaves AV, Meale SJ. In vitro screening of anti-methanogenic additives for use in Australian grazing systems. Front Anim Sci 2023;4:1123532. https://doi.org/10.3389/fanim.2023.1123532.
Passos AA, Park I, Ferket P, von Heimendahl E, Kim SW. Effect of dietary supplementation of xylanase on apparent ileal digestibility of nutrients, viscosity of digesta, and intestinal morphology of growing pigs fed corn and soybean meal based diet. Anim Nutr 2015;1:19–23. https://doi.org/10.1016/j.aninu.2015.02.006.
Qiu S, Fang Z, Wu D, Lin Y, Che L. Tryptophan supplements promote pregnancy success in mice challenged with Pseudorabies virus (PRV) by regulating the expression of systemic cytokines, immunoglobulins, PRV-specific protein profiles, and Toll-like receptors. J Med Food 2011;14:857–65. https://doi.org/10.1089/jmf.2010.1146.
Reddy VY, Desorchers PE, Pizzo SV, Gonias SL, Sahakian JA, Levine RL, et al. Oxidative dissociation of human alpha 2-macroglobulin tetramers into dysfunctional dimers. J Biol Chem 1994;269:4683–91.
Regmi PR, Ferguson NS, Zijlstra RT. In vitro digestibility techniques to predict apparent total tract energy digestibility of wheat in grower pigs. J Anim Sci 2009;87:3620–9. https://doi.org/10.2527/jas.2008-1739.
Roh TR, Chen Y, Rudolph S, Gee M, Kaplan DL. In vitro models of intestine innate immunity. Trends Biotechnol 2022;39:274–85. https://doi.org/10.1016/j.tibtech.2020.07.009.
Saunderson CL. Comparative metabolism of L-methionine, DL-methionine and DL-2-hydroxy 4-methylthiobutanoic acid by broiler chicks. Br J Nutr 1985;54:621–33. https://doi.org/10.1079/BJN19850149.
Sève B. Physiological roles of tryptophan in pig nutrition. Adv Exp Med Biol 1999;467:729–41. https://doi.org/10.1007/978-1-4615-4709-9_95.
Shen YB, Voilque´ G, Odle J, Kim SW. Dietary L-tryptophan supplementation with reduced large neutral amino acids enhances feed efficiency and decreases stress hormone secretion in nursery pigs under social-mixing stress. J Nutr 2012a;142:1540–6. https://doi.org/10.3945/jn.112.163824.
Shen YB, Voilque´ G, Kim DJ, Odle J, Kim SW. Effects of increasing tryptophan intake on growth and physiological changes in nursery pigs. J Anim Sci 2012b;90:2264–75. https://doi.org/10.2527/jas2011-4203.
Shen YB, Weaver AC, Kim SW. Effect of feed grade L-methionine on growth performance and gut health in nursery pigs compared with conventional DL-methionine. J Anim Sci 2014;92:5530–9. https://doi.org/10.2527/jas2014-7830.
Shen YB, Coffey MT, Kim SW. Effects of short term supplementation of L-tryptophan and reducing large neutral amino acid along with L-tryptophan supplementation on growth and stress response in pigs. Anim Feed Sci Technol 2015a;207:245–52. https://doi.org/10.1016/j.anifeedsci.2015.06.020.
Shen YB, Ferket P, Park I, Malheiros RD, Kim SW. Effects of feed grade L-methionine on intestinal redox status, intestinal development, and growth performance of young chickens compared with conventional DL-methionine. J Anim Sci 2015b;93:2977–86. https://doi.org/10.2527/jas2015-8898.
Shen YB, Weaver AC, Kim SW. Physiological effects of deoxynivalenol from naturally contaminated corn on cerebral tryptophan metabolism, behavioral response, gastrointestinal immune status and health in pigs following a pair-feeding model. Toxins 2021;13:393. https://doi.org/10.3390/toxins13060393.
Tian QY, Zeng ZK, Zhang YX, Long SF, Piao XS. Effect of L- or DL-methionine supplementation on nitrogen retention, serum amino acid concentrations and

blood metabolites profile in starter pigs. Asian Australas J Anim Sci 2016;29:689–94. https://doi.org/10.5713/ajas.15.0730.
Tiwari UP, Chen H, Kim SW, Jha R. Supplemental effect of xylanase and mannanase on nutrient digestibility and gut health of nursery pigs studied using both in vivo and in vitro models. Anim Feed Sci Technol 2018;245:77–90. https://doi.org/10.1016/j.anifeedsci.2018.07.002.
Trevisi P, Melchior D, Mazzoni M, Casini L, De Filippi S, Minieri L, et al. A tryptophan-enriched diet improves feed intake and growth performance of susceptible weanling pigs orally challenged with *Escherichia coli* K88. J Anim Sci 2009;87:148–56. https://doi.org/10.2527/jas.2007-0732.
Toda G, Yamauchi T, Kadowaki T, Ueki K. Preparation and culture of bone marrow-derived macrophages from mice for functional analysis. STAR Protoc 2020;2(1):100246. https://doi.org/10.1016/j.xpro.2020.100246.
Tsamandouras N, Chen WLK, Edington CD, Stokes CL, Griffith LG, Cirit M. Integrated gut and liver microphysiological systems for quantitative in vitro pharmacokinetic studies. AAPS J 2017;19(5):1499–512. https://doi.org/10.1208/s12248-017-0122-4.
Vergauwen H, Tambuyzer B, Jennes K, Degroote J, Wang W, De Smet S, et al. Trolox and ascorbic acid reduce direct and indirect oxidative stress in the IPEC-J2 cells, an in vitro model for the porcine gastrointestinal tract. PLoS One 2015;10(3):e0120485. https://doi.org/10.1371/journal.pone.0120485.
Vinyard JR, Faciola AP. Unraveling the pros and cons of various in vitro methodologies for ruminant nutrition: a review. Transl Anim Sci 2022;6(4):txac130. https://doi.org/10.1093/tas/txac130.
Weir L, Robertson D, Leigh IM, Panteleyev AA. The reduction of water-soluble tetrazolium salt reagent on the plasma membrane of epidermal keratinocytes is oxygen dependent. Anal Biochem 2011;414(1):31–7. https://doi.org/10.1016/j.ab.2011.02.030.
Weischenfeldt J, Porse B. Bone marrow-derived macrophages (BMM): isolation and applications. CSH Protoc 2008;3(12):pdb.prot5080. https://doi.org/10.1101/pdb.prot5080.
Weurding RE, Veldman A, Veen WA, van der Aar PJ, Verstegen MW. In vitro starch digestion correlates well with rate and extent of starch digestion in broiler chickens. J Nutr 2001;131:2336–42. https://doi.org/10.1093/jn/131.9.2336.
Woyengo TA, Jha R, Beltranena E, Zijlstra RT. In vitro digestion and fermentation characteristics of canola co-products simulate their digestion in the pig intestine. Animal 2016;10(6):911–8. https://doi.org/10.1017/S1751731115002566.
Wu G, Kim SW. Functional amino acids in animal production. In: Ullrey DE, Baer CK, Pond WG, editors. Encyclopedia of animal science. 2nd ed. Boca Raton: CRC Press; 2007. p. 463–6 (ISBN 9781439809327).
Wu G, Knabe DA, Kim SW. Arginine nutrition in neonatal pigs. J Nutr 2004;134:2783S–90S. https://doi.org/10.1093/jn/134.10.2783S.
Wu G, Bazer FW, Davis TA, Jaeger LA, Johnson GA, Kim SW, et al. Important roles for the arginine family of amino acids in swine nutrition and production. Livest Sci 2007;112:8–22. https://doi.org/10.1016/j.livsci.2007.07.003.
Wu X, Ruan Z, Gao Y, Yin Y, Zhou X, Wang L, et al. Dietary supplementation with L-arginine or N-carbamylglutamate enhances intestinal growth and heat shock protein-70 expression in weanling pigs fed a corn- and soybean meal-based diet. Amino Acids 2010;39:831–9. https://doi.org/10.1007/s00726-010-0538-y.
Xu X, Chang J, Wang P, Yin Q, Liu C, Li M, et al. Effect of chlorogenic acid on alleviating inflammation and apoptosis of IPEC-J2 cells induced by deoxyniyalenol. Ecotoxicol Environ Saf 2020;205:111376. https://doi.org/10.1016/j.ecoenv.2020.111376.
Xu X, Duarte ME, Kim SW. Postbiotics effects of Lactobacillus fermentate on intestinal health, mucosa-associated microbiota, and growth efficiency of nursery pigs challenged with F18+ *Escherichia coli*. J Anim Sci 2022;100:skac210. https://doi.org/10.1093/jas/skac210.
Yan H, Ajuwon KM. Butyrate modifies intestinal barrier function in IPEC-J2 cells through a selective upregulation of tight junction proteins and activation of the Akt signaling pathway. PLoS One 2017;12(6):e0179586. https://doi.org/10.1371/journal.pone.0179586.
Yin LM, Wei Y, Wang WQ, Wang Y, Xu YD, Yang YQ. Simultaneous application of BrdU and WST-1 measurements for detection of the proliferation and viability of airway smooth muscle cells. Biol Res Res 2014;47(1):75. https://doi.org/10.1186/0717-6287-47-75.
Zaefarian F, Cowieson AJ, Pontoppidan K, Abdollahi MR, Ravindran V. Trends in feed evaluation for poultry with emphasis on in vitro techniques. Anim Nutr 2021;7(2):268–81. https://doi.org/10.1016/j.aninu.2020.08.006.
Zhan Z, Ou D, Piao X, Kim SW, Liu Y, Wang J. Dietary arginine supplementation affects microvascular development in the small intestine of early-weaned pigs. J Nutr 2008;138:1304–9. https://doi.org/10.1093/jn/138.7.1304.
Zhang B, Sun H, Sun Z, Liu N, Liu R, Zhong Q. Glutamine alleviated heat-stress-induced damage of porcine intestinal epithelium associated with the mitochondrial apoptosis pathway mediated by heat shock protein 70. J Anim Sci 2023:skad127. https://doi.org/10.1093/jas/skad127.
Zhang M, Lv L, Cai H, Li Y, Gao F, Yu L, et al. Long-term expansion of porcine intestinal organoids serves as an in vitro model for swine enteric coronavirus infection. Front Microbiol 2022;13:865336. https://doi.org/10.3389/fmicb.2022.865336.
Zheng L, Duarte ME, Loftus AS, Kim SW. Intestinal health of pigs upon weaning: challenges and nutritional intervention. Front Vet Sci 2021;8:628258. https://doi.org/10.3389/fvets.2021.628258.